

# UC San Diego

## UC San Diego Electronic Theses and Dissertations

### Title

Impact of Mycobiome on Dysregulation of Inflammasome-related Genes in Head and Neck Squamous Cell Carcinomas and Lung Squamous Cell Carcinomas

### Permalink

<https://escholarship.org/uc/item/3w24s64r>

### Author

Shende, Neil Vivek

### Publication Date

2022

Peer reviewed|Thesis/dissertation

UNIVERSITY OF CALIFORNIA SAN DIEGO

Impact of Mycobiome on Dysregulation of Inflammasome-related Genes in Head and Neck  
Squamous Cell Carcinomas and Lung Squamous Cell Carcinomas

A thesis submitted in partial satisfaction of the requirements  
for the degree Master of Science

in

Biology

by

Neil Vivek Shende

Committee in charge:

Professor Weg Ongkeko, Chair  
Professor Lifan Lu, Co-chair  
Professor Enfu Hui

Copyright

Neil Vivek Shende, 2022  
All rights reserved.

The thesis of Neil Vivek Shende is approved, and it is acceptable in quality and Form for publication on microfilm and electronically.

University of California San Diego

2022

## TABLE OF CONTENTS

Thesis Approval Page.....	iii
Table of Contents.....	iv
List of Abbreviations.....	v
List of Figures.....	vi
Acknowledgements.....	vii
Abstract of the Thesis.....	viii
Chapter 1 Introduction.....	1
Chapter 2 Methods and Materials.....	8
Chapter 3 Results.....	14
Chapter 4 Discussion.....	36
Appendix.....	44
References.....	47

## LIST OF ABBREVIATIONS

Abbreviation	Description
HNSC or HNSCC	Head and Neck Squamous Cell Carcinoma
HPV	Human Papillomavirus
CDC	Centers for Disease Control
LUSC	Lung Squamous Cell Carcinoma
PAMP	Pathogen Associated Molecular Pattern
DAMP	Danger Associated Molecular Pattern
TCGA	The Cancer Genome Atlas
NCBI	National Center for Biotechnology Information
GSEA	Gene Set Enrichment Analysis
ANOVA	Analysis of Variance

## LIST OF FIGURES

Figure 1 Schematic of the project's workflow .....	16
Figure 2 Correlation of differentially abundant fungal species to sample type .....	18
Figure 3 Correlation of fungal abundance to patient survival .....	20
Figure 4 Correlation of differentially abundant fungi to clinical variables .....	22
Figure 5 Correlation of differentially expressed inflammasome-related genes to fungal abundance .....	26
Figure 6 Correlation of fungal abundance to immune cell populations .....	32
Figure 7 The association of fungal abundance to inflammasome-related pathways using GSEA .....	35

## ACKNOWLEDGEMENTS

I would like to acknowledge Dr. Weg Ongkeko for his help and support as the chair of my committee. He has supported and guided me throughout this thesis, and has encouraged me over the last four years. Thank you for being an amazing mentor and fostering teamwork and cooperation in the lab.

I would also like to acknowledge members of the Ongkeko lab who have been incredible teammates over the past four years.

I want to acknowledge Dr. Lifan Lu for his time and support in being the co-chair of the committee, and Dr. Enfu Hui for his help in being part of the committee.

You are very much appreciated.



## ABSTRACT OF THE THESIS

Impact of Mycobiome on Dysregulation of Inflammasome-related Genes in Head and Neck Squamous Cell Carcinomas and Lung Squamous Cell Carcinomas

by

Neil Vivek Shende

Master of Science in Biology

University of California San Diego, 2022

Professor Weg Ongkeko, Chair

Professor Lifan Lu, Co-chair

Cancer continues to be a lethal challenge to human health. While research has uncovered many causes and effects of cancer, the role of the microbiome has been uncovered more recently. Fungi are an integral part of the human mycobiome, yet they have been studied far less than the bacterial microbiome in cancer. Studying the immune response to fungal pathogens is an important endeavor as it can shed light on the fungal landscape in healthy and cancerous tissue. Fungal pathogenesis involves the activation of

inflammasomes and is an important aspect of the immune response to fungi. In this study I sought to characterize the fungal mycobiome in head and neck squamous cell carcinoma (HNSC) and lung squamous cell carcinoma (LUSC), and to elucidate dysregulations of inflammasome-related genes in the two cancers. I used RNA-seq data from TCGA from cancer tissue and adjacent normal tissue, extracted fungal abundance counts, and correlated these with survival, clinical variables, and infiltration of multiple types of immune cells. I also identified correlations between fungal abundance and inflammasome-related genes, and inflammasome-related pathways. I found multiple fungal species to be differentially abundant and correlated with inflammasome-related genes in both HNSC and LUSC including *Saccharomyces cerevisiae*, *Saccharomyces cerevisiae* N85, and *Kappamyces sp.* PL-117. I also found species that were uniquely associated with HNSC or LUSC. These findings characterize the fungal mycobiome and elucidate the correlation between fungal species and inflammasome-related genes in HNSC and LUSC.

## Chapter 1 Introduction

Cancers are a group of diseases that involve rapid, uncontrolled cell division.

According to the World Health Organization (WHO), there were 10 million cancer deaths worldwide in 2020. Cancer can develop in a variety of different organs and tissue types, but the majority arise from epithelial tissue. Epithelial tissues consist of sheets of cells that cover surfaces and cavities. Cancers originating from epithelial tissues are called carcinomas and are responsible for 80% of cancer-related deaths (<https://seer.cancer.gov>). Squamous cell carcinomas are cancers arising from epithelial cells that form protective layers. This study focuses on head and neck squamous cell carcinoma and lung squamous cell carcinoma.

Around the globe, there are an estimated 850,000 new cases of head and neck squamous cell carcinoma (HNSC) a year, and about half million deaths from the disease [1]. Like HNSCC, lung squamous cell carcinoma (LUSC), is a cancer that arises in the squamous cells lining the airways of the lungs. According to the Centers for Disease Control (CDC), 218,520 new cases of lung cancer were newly diagnosed in the United States in 2018, the last year for which numbers are available, and 142,080 deaths resulted from the disease [2]. Studying the risk factors associated with these cancers will be vital to developing new treatments and studying these cancers in tandem can provide further insights into their similarities and differences.

Several major risk factors of HNSC are well-documented, including alcohol consumption [3], smoking [4], and chewing betel leaves [5]. However, others are still under investigation. Recently, there has been growing interest in studying how the oral microbiome affects cancer initiation, progression, and outcomes. In a recent study from Brazil, Maria Arbelaez and colleagues found that when epithelial cells in the oral cavity were stimulated

with the fungus *Candida albicans*, the oral microbiome was altered in a manner that affected the expression of several protooncogenes and cell cycle genes resulting in a tumor-conducive environment in the oral cavity [6]. Studying the role of other fungal species in cancers of the head and neck can provide insights into not just the causes of the disease, but also therapies and outcomes.

As is true for HNSC, several risk factors of LUSC have also been identified. Among them, smoking has been long recognized as a major risk factor for lung cancer, with 80-90% of cases being related to smoking or second-hand tobacco smoke exposure [1]. However, uncovering other causes of the disease as well as understanding how the lung environment and lifestyle and other behaviors affect the disease are still being investigated. The lungs are a site of constant exposure to microbes, and many lung diseases are caused by viruses, bacteria, and other microbes. Elucidating the role of the microbiome in lung cancer is critical to creating a better understanding of the disease. Research has also shown that the host's microbiome is a critical part of regulating and activating tumorigenesis [7]. When responding to bacterial, viral, and fungal infections, the balance of oxygen levels, temperature and pH in the lungs alters leading to dynamic changes in the lungs [8]. Immune responses, including inflammation, resulting from pathogen associated molecular patterns (PAMPs) can lead to chronic inflammation and a lung environment susceptible to further damage and diseases including lung cancer [8].

The immune system is a complex defense system that protects organisms from disease. In humans, it can target and kill a variety of microbes, including bacteria, fungi, parasites, viruses, and cancer cells. The innate immune system includes anatomical barriers

such as the skin, gastrointestinal tract, lungs, and blood-brain barrier as well as defensive substances like tears, saliva, mucus, and gastric acid that keep microbes from freely accessing the inside of the body. If microbes are detected inside the body, the innate immune system can employ general responses such as the complement system response [9, 10] and the inflammation response [11, 12].

In the event of infection, irritation, or injury, one of the first responses of the innate immune system is inflammation. The inflammatory response involves redness, heat, swelling, and loss of function. One of the purposes of swelling is to produce a physical barrier against infection, and the heat produces an environment that is not conducive to the growth of microbes. Inflammation is an extremely important early response that attempts to limit the damage tissue caused by the initial stimulus. An innate immune response can occur as a response to tumors when dying cancer cells release substances recognized as danger-associated molecular patterns (DAMPs) [13]. However, abnormal inflammatory responses can lead to several disorders, including allergic reactions, pneumonia, autoimmune diseases, asthma, colitis, inflammatory bowel disease, and rheumatoid arthritis. Chronic inflammation is also associated with the development of cancer [14]. Inflammation induces the production of reactive oxygen species (ROS) [15] and reactive nitrogen species (RNS) [16] in order to fight infection. However, reactive oxygen species and reactive nitrogen species can cause DNA damage, which can lead to mutations and epigenetic alterations. Mutations acquired during periods of chronic inflammation can lead to the development of cancer.

Inflammasomes are multiprotein complexes that are responsible for the activation of the inflammatory response. They activate and assemble in response to pathogen-associated

molecular patterns (PAMPs) or danger-associated molecular patterns (DAMPs). When the pattern recognition receptor (PRR) of the inflammasome detects a PAMP or DAMP, a caspase activation and recruitment domain (CARD) will bind pro-caspase-1 [17]. The CARD can be of the inflammasome itself or of the adaptor protein ASC. When the inflammasome is fully assembled, it will bring together many pro-caspase-1 molecules. These molecules will then catalyze their own cleavage and assemble into active caspase-1. Caspase-1 induces maturation of interleukin 18 (IL-18) and interleukin 1 $\beta$  (IL-1 $\beta$ ) by cleaving pro IL-18 and pro IL-1 $\beta$ . IL-18 and IL-1 $\beta$  are cytokines that promote the inflammatory response [18].

Caspase 1 also cleaves gasdermin D, which induces swelling and cell lysis [19]. This inflammatory programmed cell death is called pyroptosis. Pyroptosis is used to stop the replication of intracellular pathogens and can also release inflammatory cytokines from the cell [20]. Studies have shown that the NLRP3 inflammasome activation is associated with oncogenesis in head and neck cancer [21], and that the AIM2 inflammasome is upregulated in non-small cell lung cancer [22]. Further, caspase-1, IL-1 $\beta$ , and IL-18 are overexpressed in lung cancer tissue [23]. Due to the importance of inflammasomes to inflammation and programmed cell death, the dysregulation of inflammasome genes is frequently observed in cancer.

In both HNSCC and LUSC, the environment surrounding a tumor, or tumor microenvironment, can have a substantial impact on cancer outcomes. An important aspect of the tumor microenvironment is the presence of immune system signaling molecules and tumor-infiltrating immune cells. The presence of many types of tumor-infiltrating immune cells have been shown to be predictive of better cancer outcomes [24]. Signaling molecules can induce immune responses such as inflammation, and influence regulation of

inflammasome genes [25, 26]. Tumors can influence the immune response by sending signals and inducing immune tolerance. [27, 28]. The microbiome can also have a substantial impact on the tumor microenvironment. Studying the microbial landscape of cancers is therefore imperative to understanding the mechanisms that drive them.

The human microbiome is a collection of microorganisms that inhabit human tissues. These microorganisms include bacteria, archaea, viruses, fungi, and other eukaryotes. Fungi are unicellular or multi-cellular eukaryotic organisms that are organized in their own kingdom and include microorganism such as yeasts and molds. The fungal microbiome, or mycobiome, consists of fungal species that inhabit the oral cavity, gut, and other body sites. There have been fewer studies documenting the species of fungi present in the mycobiome compared with bacterial species in the bacterial microbiome. However, recent studies have shown multiple fungal species present in the oral microbiome including *Candida*, *Fusarium*, *Mycosphaerella* and *Saccharomyces* [29]. Compared to the oral mycobiome, the lung mycobiome has been shown to have greater diversity of species. Variety of species including *Cladosporium*, *Eurotium*, *Penicillium*, *Aspergillus*, *Candida*, *Malassezia*, and *Pneumocystis* have been found in the lung and respiratory tract [30]. Similar species of fungi have been found in both the oral cavity and during bronchoalveolar lavage in healthy individuals [31]. This suggests that there may be overlaps in fungal species in the oral cavity, upper and lower respiratory tracts. Studying the composition of the fungal microbiome in the head, neck, oral, respiratory and lung cavities will provide a fuller picture of the microbes and their role in health and disease.

Few studies have investigated the connection between fungi and cancer. However, in a study in 2019, researchers found that the fungal species *Malassezi* found more abundantly in

the patients with pancreatic cancer was responsible for tumor growth. They found this by injecting mice with four different types of fungi, and observing that mice injected with *Malassezi* had accelerated growth of their malignancies [32]. Studies have also linked *Candida albicans* and *Malassezi* with cervical cancer [33]. Further studies investigating the correlation between the mycobiome, and cancer can provide valuable insights for prevention, diagnosis, and treatment of the disease. Fungi have also been associated with the immune response and gene expression. *Candida albicans*, for instance, sometimes acts as a commensal species, and at other times switches to a pathogenic form. In a 2019 study, Wang et. al. found that *Candida albicans* upregulated the protein Sell which in turn activates the NF-kB and MAPK pathways [34]. Fungal species, including *Candida albicans*, have been shown to promote inflammation [35] and induce a Th17 response [36, 37]. While we are beginning to investigate the pathogenic fungi, few studies have investigated the full landscape of fungal pathogens, their role in diseases such as cancer or their correlations to inflammasome-related genes.

Recently, there has been growing interest in studying how the oral microbiome affects cancer initiation, progression, and outcomes. In a recent study from Brazil, Maria Arbelaez and colleagues found that when epithelial cells in the oral cavity were stimulated with the fungus *Candida albicans*, the oral microbiome was altered in a manner that affected the expression of several protooncogenes and cell cycle genes resulting in a tumor-conducive environment in the oral cavity [6]. Studying the role of other fungal species in cancers of the head and neck can provide insights into not just the causes of the disease, but also therapies and outcomes. The lungs are a site of constant exposure to microbes, and many lung diseases are caused by viruses, bacteria, and other microbes. Elucidating the role of the microbiome in



lung cancer is critical to creating a better understanding of the disease. Research has also shown that the host's microbiome is a critical part of regulating and activating tumorigenesis [7]. When responding to bacterial, viral, and fungal infections, the balance of oxygen levels, temperature and pH in the lungs alters leading to dynamic changes in the lungs [8]. Immune responses, including inflammation, resulting from pathogen associated molecular patterns (PAMPs) can lead to chronic inflammation and a lung environment susceptible to further damage and diseases including lung cancer [8].

In this study, I investigated the fungal microbiome in head and neck squamous cell carcinoma and lung squamous cell carcinoma to characterize the fungal landscape in these cancers. Due to the importance of inflammasome genes to the innate immune response to microbes, and to the development of and response to cancer, I hypothesized that the fungal microbiome would influence cancer outcomes by dysregulating inflammasome-related genes. I found fungi that were differentially abundant in cancer tissue compared to normal tissue. Next, I investigated the associations between fungal abundances and patient survival and clinical variables. This allowed me to focus on fungi that I suspected could be influencing cancer outcomes. Finally, to characterize the relationship between the fungal microbiome and the inflammation response, I investigated the correlations between fungal abundance and the expression of inflammasome-associated genes. I further studied the association between the fungal microbiome and the immune system by examining the relationship between fungal abundances and immune infiltration and the enrichment of immune-associated gene sets.

## Chapter 2 Materials and Methods

### *Data acquisition from The Cancer Genome Atlas (TCGA)*

TCGA is a database of multi-omics data including gene expression, miRNA expression and DNA methylation data for multiple cancer types. In addition to gene expression data, corresponding clinical data is also available. This makes it possible to study gene expression and the microbial species landscape in the context of patient clinical variables. For this reason, RNA-sequencing data from TCGA was used in this study. Raw whole-transcriptome RNA-sequencing data was downloaded for head and neck squamous cell carcinoma (HNSC) and lung squamous cell carcinoma (LUSC) cancers. Primary tumor data was obtained for 513 HNSC patients and 448 LUSC patients. Additionally, 41 samples of adjacent normal tissue data was downloaded from HNSC patients, and 51 samples of adjacent normal tissue data was downloaded from LUSC patients from the TCGA legacy archive (<https://portal.gdc.cancer.gov/>). HNSC data was downloaded on 30 June 2021 while LUSC data was downloaded on 20 September 2021. Clinical information for all patients were downloaded from the Broad GDAC FireBrowse (<http://firebrowse.org/>, Date accessed: 20 October 2021) site. All data was downloaded to San Diego Supercomputer Center's (SDSC) Expanse computer cluster for extraction of gene expression data as well as fungal species abundance data.

### *Extraction of fungal reads and computation of fungal abundance*

Pathoscope 2.0 [38] is a bioinformatics pipeline capable of identifying reads from fungal strains present in RNA-sequencing data. The tool is capable of extracting the

reference genome library, performing read alignment and quality control, strain identification, and annotation of results. Thus, Pathoscope 2.0 was used to filter the RNA-sequencing data for fungal reads via direct alignment through a wrapper for Bowtie2. Fungal sequences available through the NCBI (National Center for Biotechnology Information) nucleotide database (<https://www.ncbi.nlm.nih.gov/nucleotide/>) were used as a reference genome. Pathoscope provides results in the form of two measures to quantify the amount of fungal species in a sample. The Best Hit measure denotes the absolute integer count of each species in the sequencing data, while the Best Guess measure denotes the relative abundance of each species as a percentage. In the study, the Best Hit measure was used to quantify the fungal abundance in each sample. A combined matrix of Best Hit data from all fungal species present in all samples was compiled.

To address the concerns of heterogeneity and irregularity of TCGA data, normalization was performed on the combined matrices. First, the quality of the metadata was assessed to remove samples with missing values for metadata variables including age, race and FFPR status. Next, the Voom algorithm was used to logarithmically transform the raw fungal read counts into log counts per million (CPM) data. Weighted trimmed mean of M-values (TMM) normalization was used for all data by the Voom algorithm [39].

#### *Contamination correction*

External and internal contamination are the two main categories of contamination of RNA-sequencing data. Patient tissue samples handled in the most stringent protocols

can still have microbial species not arising from the patient sample itself. This remains a major challenge in studying the microbiome and microbial landscape in tissue and blood samples. Contamination may arise from multiple sources and identifying and removing contaminants is vital to reducing errors in characterizing the true microbial landscape. External contamination usually arises from outside sources such as technicians' bodies, laboratory work surfaces, and devices and instruments used to collect and process samples. Internal contamination normally results from the samples themselves being mixed with each other during laboratory procedures. In order to minimize the impact of such contamination on the results, a multi-pronged approach was used. The goal of this approach was to identify and remove external contaminants, characterize internal contaminants, and estimate the impact on the data. First, a literature search was performed to identify common laboratory fungal contaminants. I then proceeded to remove these contaminant species from the data of microbial abundance. Following this, the *decontam* package in R [40] was used to identify and remove potential contaminants in the tissue data.

#### *Differential fungal abundance between cancer and normal samples*

In order to compare fungal abundance in cancer versus normal samples, differential abundance analysis was performed. Fungal species present in fewer than 10 samples, per cancer, were removed from the analysis. Further, samples of `sample_type` metastatic were also removed from consideration, leaving samples that were either classified as primary tumor or solid tissue normal for further analysis. The Kruskal-Wallis test, a one-way ANOVA analysis of variance, was performed separately on HNSC

and LUSC patient data to determine differential abundance. The R function `kruskal.test` was used to perform the test, with results considered significant if  $p < 0.05$ .

#### *Microbial abundance correlation to patient survival*

Survival analysis was undertaken by establishing the relationship between differentially abundant fungal species and patient survival using the Kaplan-Meier test. The main goal of this analysis was to determine whether there was a difference in the survival of patients based on the differences in fungal abundance. Fungal abundance was represented as a binary variable for each fungal species. The two possible values were high abundance, or values above the median, and low abundance, which were values below the median abundance value. Cox regression analysis was used to determine which differentially abundant fungal species are significantly correlated with HNSC and LUSC patient survival based on a cutoff of  $p < 0.05$ .

#### *Correlation of fungal abundance to clinical variables*

In order to investigate the differences in fungal abundance across clinical variables in cancer samples, the Kruskal-Wallis test was used. Relevant variables including age, gender, neoplasm histologic grade, pathologic state, HPV status, and smoking and alcohol history were examined. For pathologic stage T, N, and M, samples that were assigned intermediate stages such as t1a, t1b or t1 c, were grouped into the stage t1. Similar consolidation was carried out for all three pathologic stage variables. Indeterminate pathologic stage samples were removed from consideration for this clinical variable analysis. For the clinical variable frequency of alcohol consumption, data was grouped into quartiles producing four categories for comparison. The clinical data for these comparisons was downloaded from the FireBrowse database (<http://firebrowse.org/>),

Date accessed: 20 October 2021). Associations between fungal abundance and clinical variables were deemed significant if  $p < 0.05$ .

*Differential expression analysis to determine dysregulated immune-associated and inflammasome-related genes*

In order to perform differential expression analysis, DESeq2 [41] was used. mRNA read counts were filtered, and lowly expressed mRNAs (counts per million  $< 1$  when comparing larger groups to smaller groups in a cohort) were removed. A counts per million matrix was produced, and mRNAs were considered to be significantly dysregulated if they had a fold change  $> |2|$  and a false discovery rate (FDR)  $< 0.05$ . After the analysis significant genes that were deemed to be immune associated and inflammasome related, were retained. Both immune associated and inflammasome associated genes were further considered to better understand the entire immune landscape of fungal abundance and gene correlations. A list of inflammasome-related genes was compiled from reviewing literature as well as from the MSigDB collections' [42, 43] C7 immunologic signatures gene set database. The list of inflammasome-related genes used in the analyses is provided in Table S3.

Using results from gene expression data and fungal abundance values, correlations were sought using the Spearman's Rank Correlation. A gene was considered to be significantly correlated to fungal abundance of a species if  $p < 0.05$ .

*Correlation of Fungal Abundance to Immune Infiltration*

The CIBERSORTx [44] tool was used to calculate the estimated relative immune cell infiltration levels for 22 cell types. CIBERSORTx is a digital cytometry tool that allows calculation of cell type abundance in bulk tissue data. It uses a reference matrix to

make an estimation of cell abundance in given samples. The “Impute Cell Fractions” feature was used to determine relative cell levels. Fungal abundance was then correlated with immune cell infiltration levels for each fungal species. Fungal abundance was set as a high (above median) and low (below median). Naïve B-cells, memory B-cells, plasma cells, CD8 T-cells, CD4 naïve T-cells, CD4 memory resting T-cells, CD4 memory activated T-cells, follicular helper T-cells, regulatory T-cells, gamma-delta T-cells, resting NK cells, activated NK cells, monocytes, M0-M2 macrophages, resting dendritic cells, activated dendritic cells, resting mast cells, activated mast cells, eosinophils, and neutrophils were examined.

#### *Correlation of Fungal Abundance to Inflammasome-Related Pathways*

Gene Set Enrichment Analysis (GSEA) software [43] was used to identify fungi associated with dysregulation of inflammasome-related pathways. Microbes with less than half non-zero values were eliminated, while those with more than half non-zero values were inputted as a continuous variable for the phenotype file. The log counts per million (CPM) file with gene expression values was used for the expression file. Next, microbe abundance was correlated to gene expression using Pearson correlations for the continuous phenotype data. Four inflammasome related pathways were studied to specifically find gene sets of significance. These pathways were downloaded from the Molecular Signatures Database [42], and included REACTOME\_INFLAMMASOMES [45] and REACTOME\_THE\_NLRP3\_INFLAMMASOME [46]. A  $p < 0.05$  threshold was used to define significant pathways.

## Chapter 3 Results

### *Data acquisition and extraction of fungal reads*

TCGA mRNA sequencing data was processed through Pathoscope 2.0 to align and quantify fungal species reads for head and neck squamous cell carcinoma (HNSC) and lung squamous cell carcinoma (LUSC) patient tissue samples (Figure 1). All samples were collected during surgery with no prior treatment such as chemotherapy, radiation, or immunotherapy. A total of 555 HNSC and 539 LUSC samples were downloaded. Of these, 513 primary tumor samples and 41 solid tissue normal samples of HNSC were included for further analysis, while 1 metastatic tumor sample was not included. In addition, 488 primary tumor samples and 51 solid tissue normal samples of LUSC were also included. A reference file was created from the NCBI database for all fungal species available. After performing Pathoscope alignment and quantification, a combined matrix of the Best Hit values was compiled consisting of microbe abundance for 9,360 fungal species for HNSC, and 9,738 fungal species for LUSC. The Best Hit data was normalized using the Voom function in R to create a log transformed file with counts.



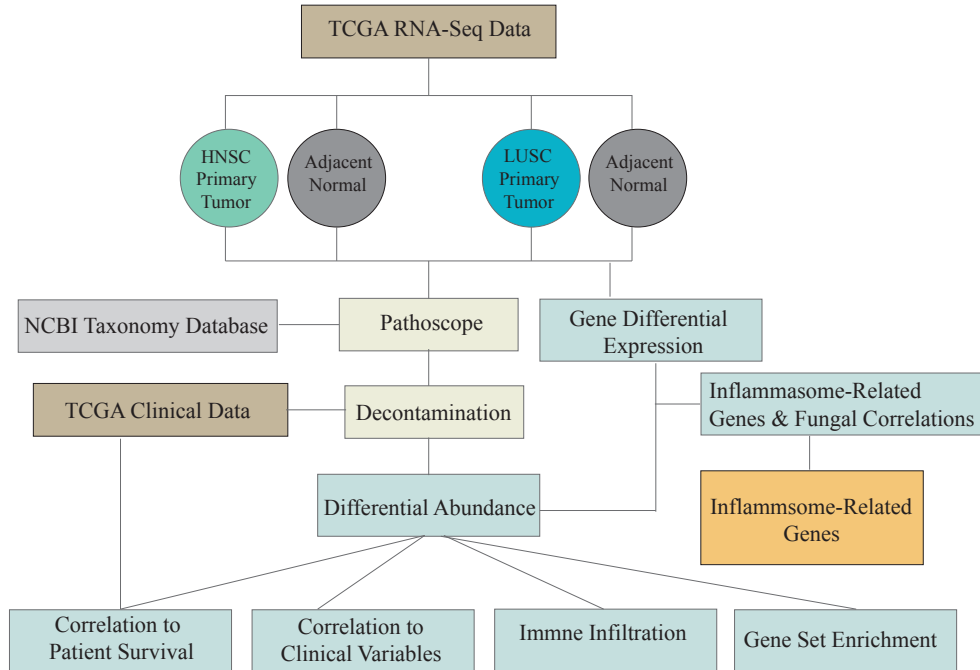


Figure 1 Schematic of the project’s workflow. Data were obtained from The Cancer Genome Atlas (TCGA) for head and neck squamous cell carcinoma (HNSC) and lung squamous cell carcinoma (LUSC) tumor and adjacent solid tissue normal samples. Fungal species information was downloaded from the National Center for Biotechnology Information’s (NCBI) taxonomy database and used to extract data through Pathoscope software.

### Contamination Correction

Contamination in TCGA RNA-seq data can arise from internal or external contaminants. Contamination corrections methods used to remove contamination bias included multiple steps. First, a literature search was performed to classify and remove known fungal contaminants in laboratory settings. Using this information, fungal contaminant species including *Rhizopus*, *Fusarium*, and *Cladosporium* [47, 48] were removed from further analysis [47, 48]. In addition, seven species of the genus were also removed (Table S1). Next, the R package *decontam* [49] was used to identify and remove contaminants from the data with a threshold of 0.1. A total of 35 species (Table S2) were identified as potential contaminants through this process and removed from the data. By

meticulously identifying and removing potential contaminants, the overall bias of these fungal species on the results was reduced.

#### *Differential fungal abundance between cancer and normal samples*

Fungi that are associated with cancer progression may have different abundances in cancer tissue than they do in normal tissue. I used the Kruskal-Wallis test to analyze the relationship between the distribution of fungal abundances and the presence or absence of cancer. Fungi were considered significantly differentially abundant if  $p < 0.05$ . In all, 33 fungi were found to be significantly differentially abundant in HNSC tumor samples compared with adjacent normal tissue. Of these, only two fungi had higher abundances in normal tissue compared with cancer tissue, and 31 had higher abundances in cancer tissue compared with normal tissue. Fifty-one fungi were found to be significantly differentially abundant in LUSC tumor samples compared with adjacent normal tissue. Of these, 18 fungi had higher abundances in normal tissue compared with cancer tissue, and 33 had higher abundances in cancer tissue compared with normal tissue.

Four fungi were significantly differentially abundant in both HNSC and LUSC: *Saccharomyces cerevisiae*, *Kappamyces sp. PL-117*, *Saccharomyces cerevisiae N85*, and *Microallomyces dendroideus* (Figure 2). *Microallomyces dendroideus*, *Saccharomyces cerevisiae N85*, and *Kappamyces sp. PL-117* all have lower abundance in normal tissue compared to cancer tissue in both LUSC and HNSC. *Saccharomyces cerevisiae* has lower abundance in cancer tissue compared with normal tissue. Thus, of the four fungi significantly differentially abundant in both HNSC and LUSC, all are differentially abundant in a direction that is consistent between the two cancers.

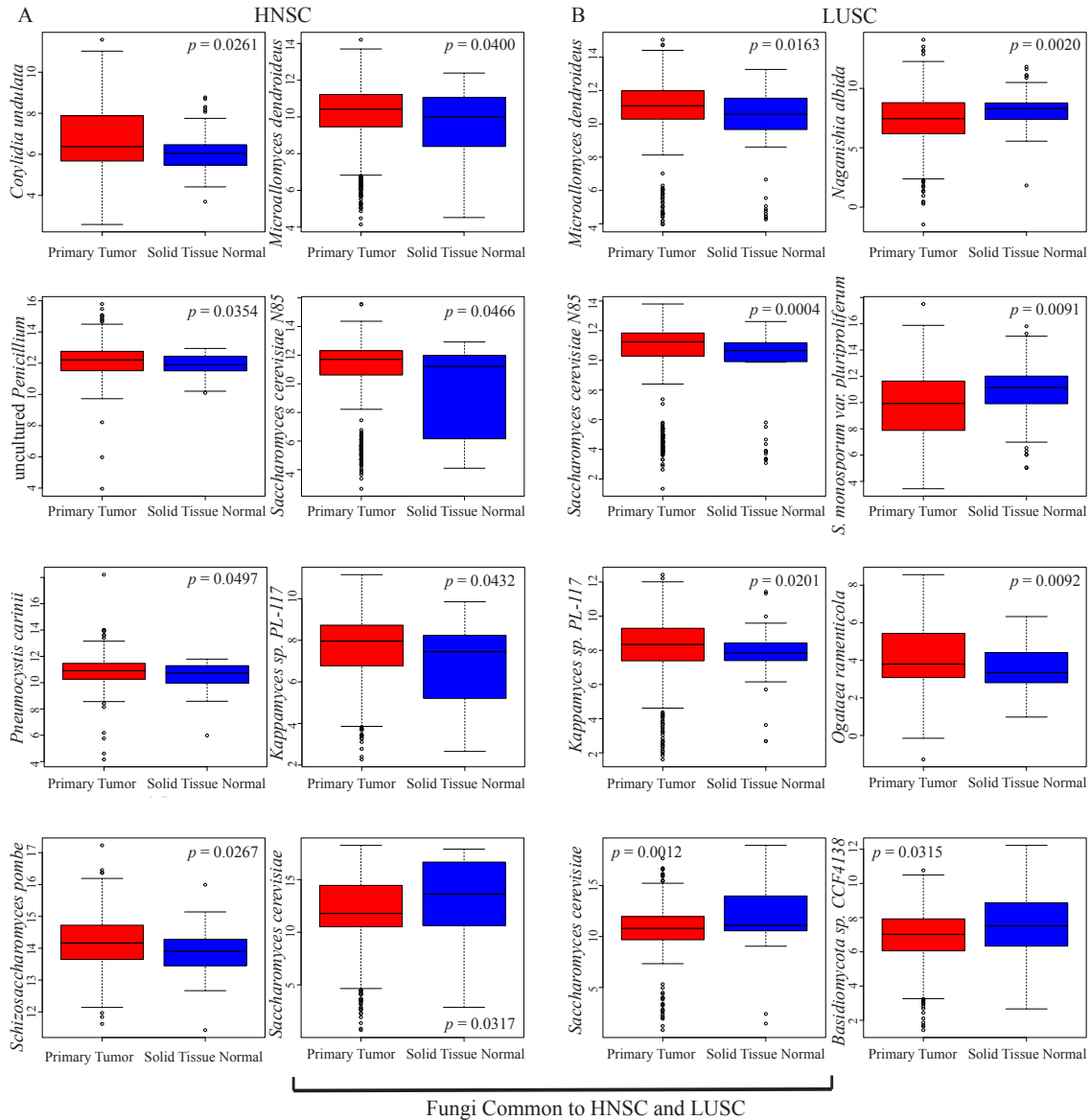


Figure 2 Correlation of differentially abundant fungal species to sample type. (A) Box plots showing correlation of fungal abundance to sample type primary tumor and solid tissue normal for HNSC patients. (B) Box plots showing correlation of fungal abundance to sample type primary tumor and solid tissue normal for LUSC patients. Outliers are represented by  $\circ$ . Box plots were created using Kruskal-Wallis Test with  $p < 0.05$  considered to be significant.

### Correlation of fungal abundance to patient survival

A fungus that is more abundant or less abundant in cancer tissue than normal tissue may not necessarily be associated with cancer outcomes. Therefore, I used Cox

Regression to determine the relationship between fungal abundance and patient survival. Fungal abundance was considered to be significantly associated with survival if  $p < 0.05$ . In HNSC, 38 fungi were found to be significantly associated with patient survival. Of these, 36 fungi tended to be present in lower abundances in patients with higher survival, and two fungi tended to be present in higher abundances in patients with higher survival. Four of the fungi that were significantly associated with patient survival were also significantly differentially abundant. These were *Schizosaccharomyces pombe*, *Cotylidia undulata*, an uncultured *Penicillium*, and *Pneumocystis carinii*. All four of these fungi tended to have higher abundances in patients with lower survival and had higher abundances in cancer tissue than normal tissue (Figure 3A).

In LUSC, 15 fungi were found to be significantly associated with patient survival. Of these, six fungi tended to be present in lower abundances in patients with higher survival, and nine fungi were present in higher abundances in patients with higher survival (Figure 3B). Three fungi, *Saccharomyces cerevisiae* N85, *Zygosaccharomyces bailii* CLIB 213, and *Inosperma maculatum* were significantly differentially abundant and associated with survival in LUSC. All three fungi had higher abundances in patients with lower survival and had higher abundances in cancer tissue compared with normal tissue.

There were fungi associated with patient survival in both cancers. However, a greater variety of fungi were associated with survival of HNSC patients than that of LUSC patients. Almost all fungi associated with survival of HNSC patients had higher abundances in patients with lower survival rates. In contrast, there were substantial portions of fungi associated with survival of LUSC patients with higher abundances and

lower abundances in patients with lower survival rates. This indicates that beneficial fungi may play a larger role in LUSC survival than HNSC survival.

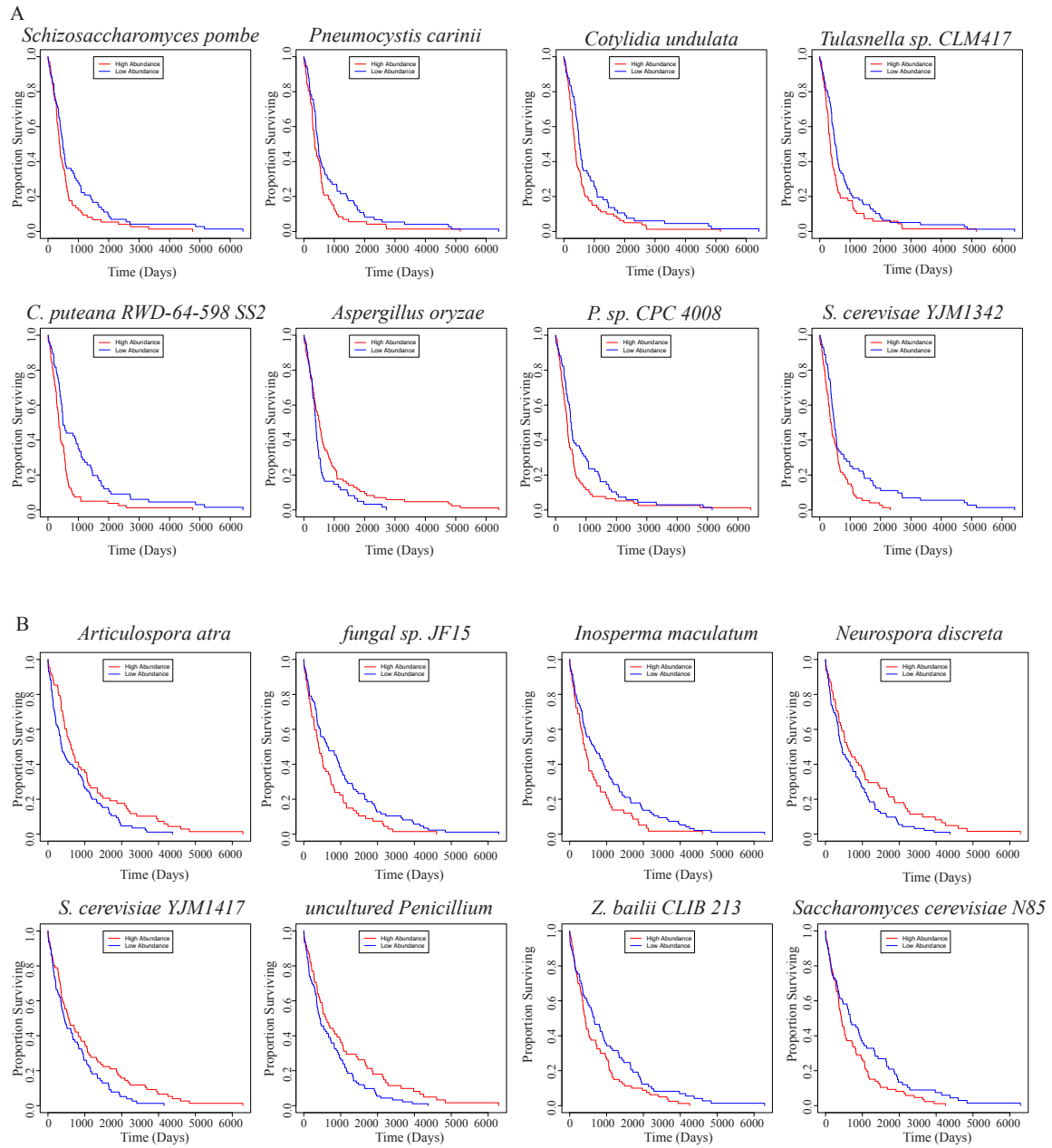


Figure 3 Correlation of fungal abundance in HNSC and LUSC cohorts to patient survival. **(A)** Kaplan–Meier plots of fungal abundance in HNSC samples to patient survival. **(B)** Kaplan–Meier plots of fungal abundance in LUSC samples to patient survival. The Cox proportional hazards regression model ( $p < 0.05$ ) was used to determine fungi correlated with survival.

### *Correlation of fungal abundance to clinical variables*

There are many aspects of cancer outcomes other than patient survival. Clinical variables can describe aspects of the cancer such as tumor size, metastasis, and spread to lymph nodes. I then used the Kruskal-Wallis test to examine the association between fungal abundances and nine clinical variables. Fungal abundances were considered significantly associated with a clinical variable if  $p < 0.05$ . The clinical variables examined were pathologic T, pathologic N, pathologic M, neoplasm status, race, gender, tobacco/smoking history, alcohol consumption, and HPV status. Fungal abundances in HNSC samples were tested against all nine variables. LUSC samples did not have data available on alcohol consumption and HPV status, so fungal abundances were only tested against the other seven variables.

In HNSC samples, alcohol consumption data was separated into four categories by dividing into quartiles. The quartiles for the dataset were 1, 6 and 7 for the first, second and third quartiles. For HNSC, the greatest number of fungi had significant associations with alcohol consumption at 53. Forty-one fungi were significantly associated with tobacco/smoking history, 40 with HPV status, 30 with pathologic N, 21 with race, and 20 with neoplasm status. No fungi were found to be significantly associated with pathologic M, pathologic M, or gender (Figure 4A). *Saccharomyces cerevisiae* N85, a differentially abundant fungi, was correlated with HPV status. *Schizosaccharomyces pombe*, another differentially abundant fungi, was also found to be correlated to HPV status and smoking/tobacco use. This fungus was also found to be significantly associated with patient survival. *Pseudogymnoascus destructans* 20631-21, which was previously found to be associated with patient survival, was also found to be

associated with HPV status and alcohol consumption. *Kappamyces sp. PL-117* and *Teratosphaeria gauchensis*, both differentially abundant fungi, were found to be associated with pathologic N. *Teratosphaeria gauchensis* was also significantly correlated with alcohol consumption. *Lachanea thermotolerans*, previously correlated with survival, was also found to be correlated with pathologic N (Figure 4B).

In LUSC samples, the greatest number of fungi had significant associations with race at 141. Ninety-eight fungi were significantly associated with tobacco/smoking history, 59 with pathologic N, 41 with neoplasm status, and 13 with pathologic T. The fewest fungi were significantly associated with pathologic M and gender at 11 each (Figure 4A). Uncultured *Cryptomycota* and *Zygosaccharomyces bailii CLIB-213* were differentially significantly abundant fungi associated with pathologic N. In addition, Uncultured *Cryptomycota* was also correlated to patient smoking/tobacco use, whereas *Zygosaccharomyces bailii CLIB-213* was also correlated with patient race. It was also correlated with patient survival. *Neurospora discreta*, previously found to be differentially significantly abundant was also correlated with survival and pathologic N. *Naganishia albida* was found to be associated with survival, and with race, while *Saccharomyces cerevisiae N85* was not only differentially significantly abundant, but also correlated to patient survival and race. *Zygosaccharomyces rouxii* was differentially significantly abundant fungi correlated with pathologic M (Figure 4C).

Race, gender, and tobacco/smoking history tended to play a larger role in the fungal microbiome of tumors in LUSC patients than in HNSC patients. In contrast, alcohol consumption and HPV status tended to play a larger role in the fungal microbiome of tumors in HNSC than in LUSC.

Figure 4 Correlation of differentially abundant fungi to clinical variables. (A) Bar plot of the number of fungi correlated to clinical data including pathologic T, pathologic N, pathologic M, neoplasm status, race, gender, smoking/tobacco history, and frequency of alcohol consumption. (B) Box plots showing correlation of fungi to pathologic N and HPV status for HNSC cancer samples. (C). Box plots showing correlation of fungi to Pathologic N, race, and Pathologic M for LUSC cancer samples. Outliers are represented by °. Box plots were created using Kruskal-Wallis Test with  $p < 0.05$  considered to be significant.



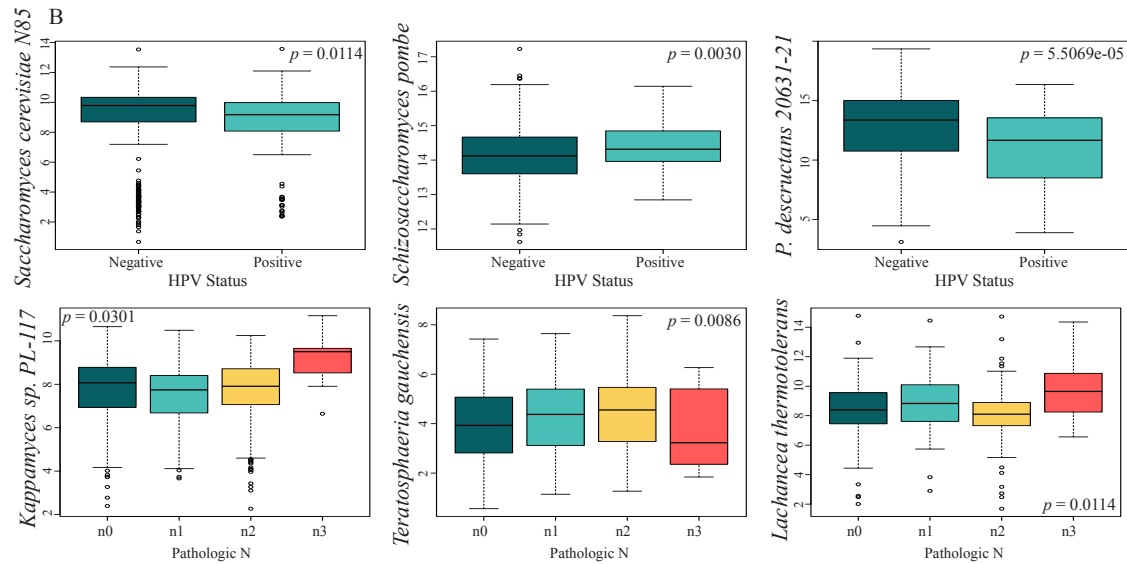
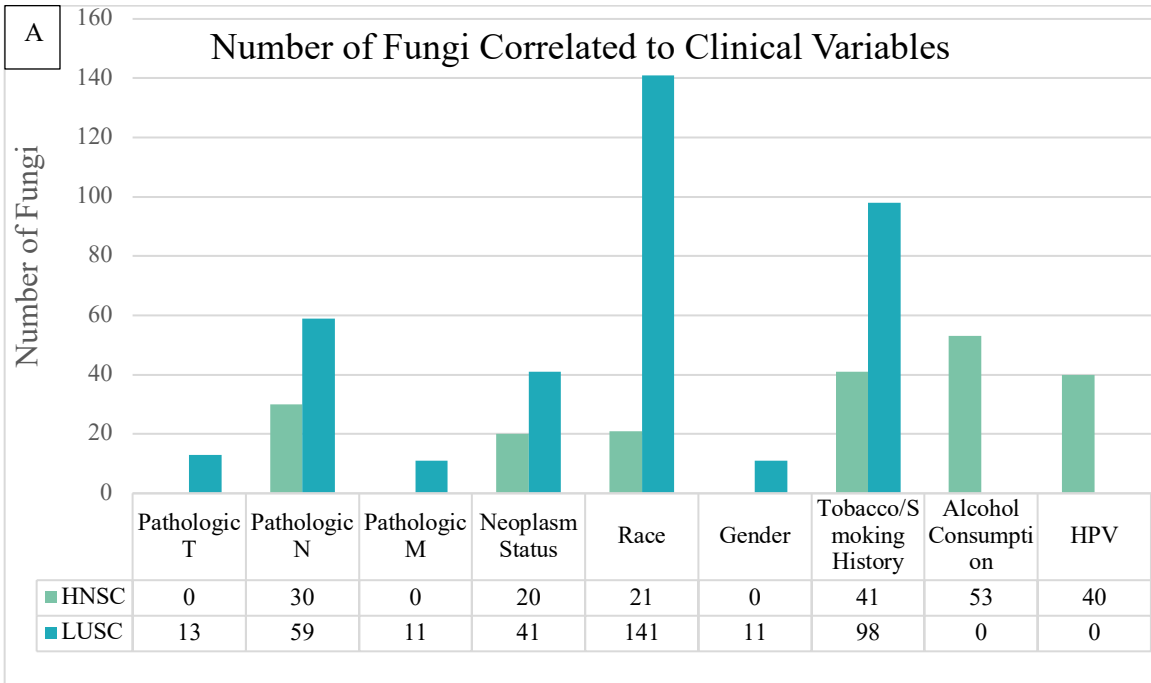
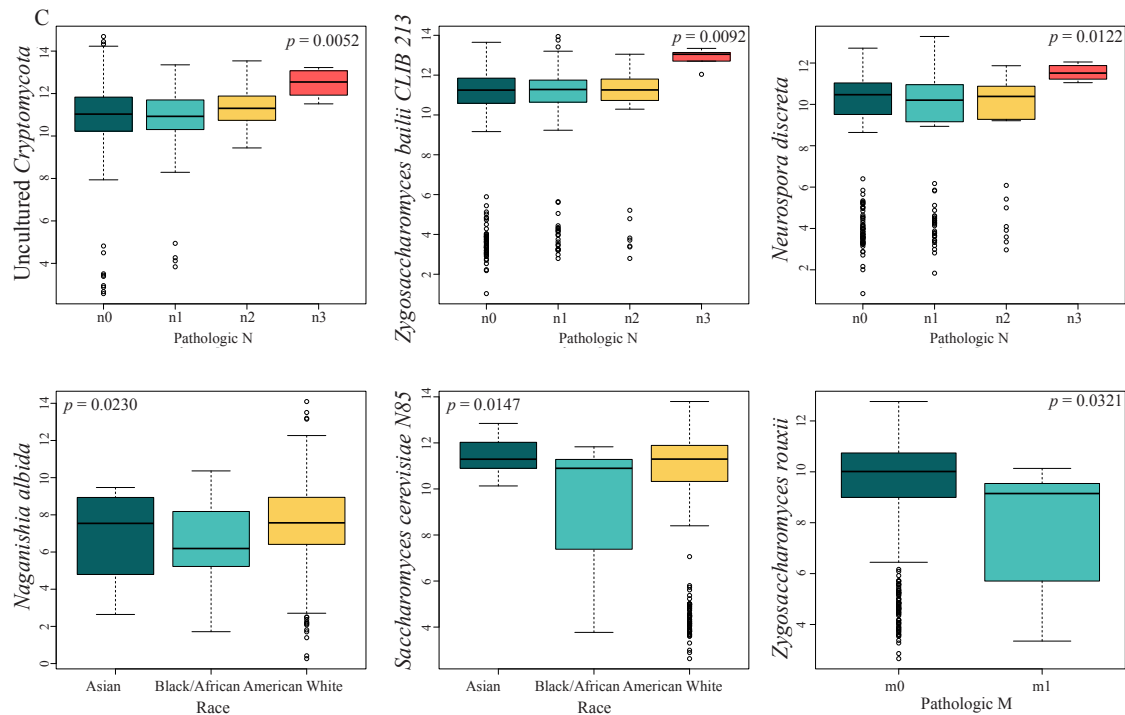


Figure 4 continued



### Correlation of Fungal Abundance to Significant Genes

Inflammasome-associated genes are very commonly dysregulated in cancer. Having found fungi significantly associated with different types of cancer outcomes, I wanted to investigate if the dysregulation of inflammasome genes could explain these associations. I used Spearman's rank correlation to find monotonic relationships between fungal abundances and the expressions of inflammasome-associated genes (Table S3). There were 26 inflammasome-associated genes correlated with the abundances of at least 20 fungi between both cancers. These genes are AIM2, APP, CASP, CASP4, CASP7, CIITA, HSP90AB1, IFI16, IL18, IL1RL1, IL33, MEFV, NAIP, NLRC4, NLRC5, NLRP1, NLRP12, NLRP2, NLRP3, NLRP6, NLRP7, PSTPIP1, TLR7, TNF, TOLLIP, and TXN (Figure 5A).

The five genes correlated with the greatest number of fungi in HNSC samples were APP with 179 fungi, TXN with 155 fungi, CASP with 93 fungi, NAIP with 70 fungi, and NLRP6 with 66 fungi. APP expression was positively correlated with abundance of both *Saccharomyces cerevisiae* and *Saccharomyces cerevisiae* N85. TXN was positively correlated with the abundance of *Kappamyces sp. PL-117*. *Schizosaccharomyces pombe* was a fungal species found to be correlated with the expression of several genes. It was negatively correlated with the expression of CASP4 and NLRP1, and positively correlated with the expression of NLRP6 (Figure 5B).

The five genes correlated with the greatest number of fungi in LUSC samples were IL1RL1 with 166 fungi, IL33 with 86 fungi, NLRC4 with 79 fungi, NLRP2 with 74 fungi, and CIITA with 57 fungi (Figure 5A). IL33 expression was positively correlated with abundance of *Hyaloraphidium curvatum*. The same fungus was also negatively correlated with expression of TXN. NLRC4 was positively correlated with abundance of *Ogateae ramenticola*. TXN expression was also positively correlated with abundance of *Kappamyces sp. PL-117* (Figure 5C).

Both HNSC and LUSC samples had positive and negative correlations between fungal abundances and expression of inflammasome genes, which is consistent with the hypothesis that fungi influence cancer outcomes by dysregulating inflammasome genes.

Figure 5 Correlation of differentially expressed inflammasome-related genes to fungal abundance. (A) Bar plot of the number of fungi correlated with inflammasome-related genes. Inflammasome-related genes with a minimum of 20 correlated fungi included in the plot. (B) Scatter plots showing correlation of inflammasome-related genes to fungal abundance for HNSC cancer samples. (C) Scatter plots showing correlation of inflammasome-related genes to fungal abundance for LUSC cancer samples. Each ° represents a tissue sample. Lines on the plot are lines of best fit. Significant correlations determined by  $p < 0.05$ .

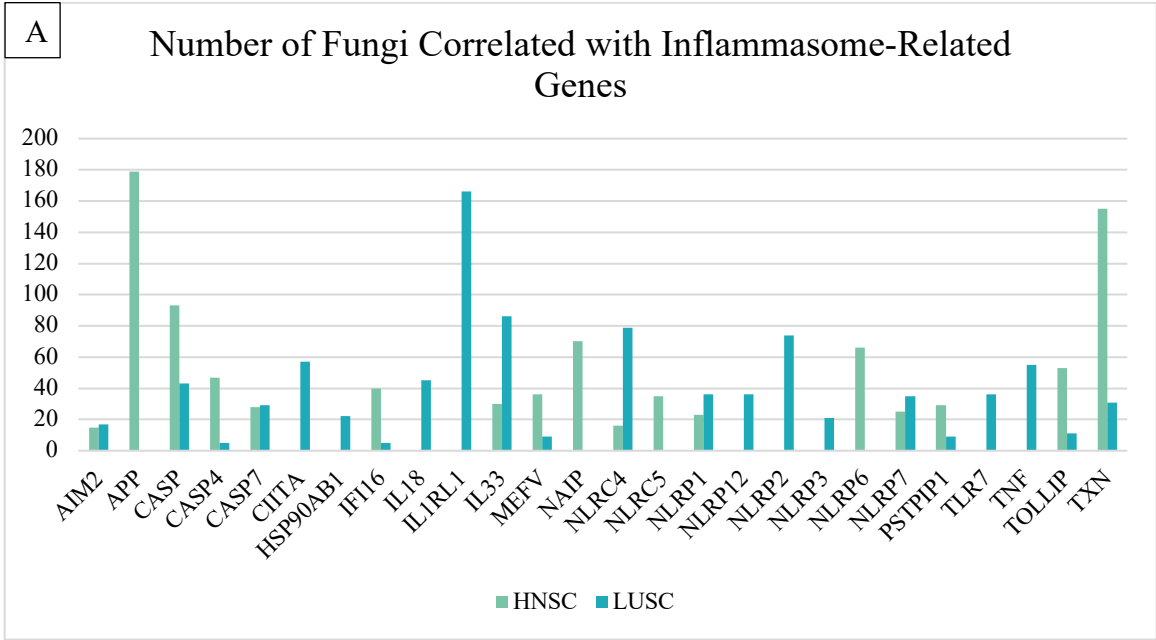


Figure 5 continued

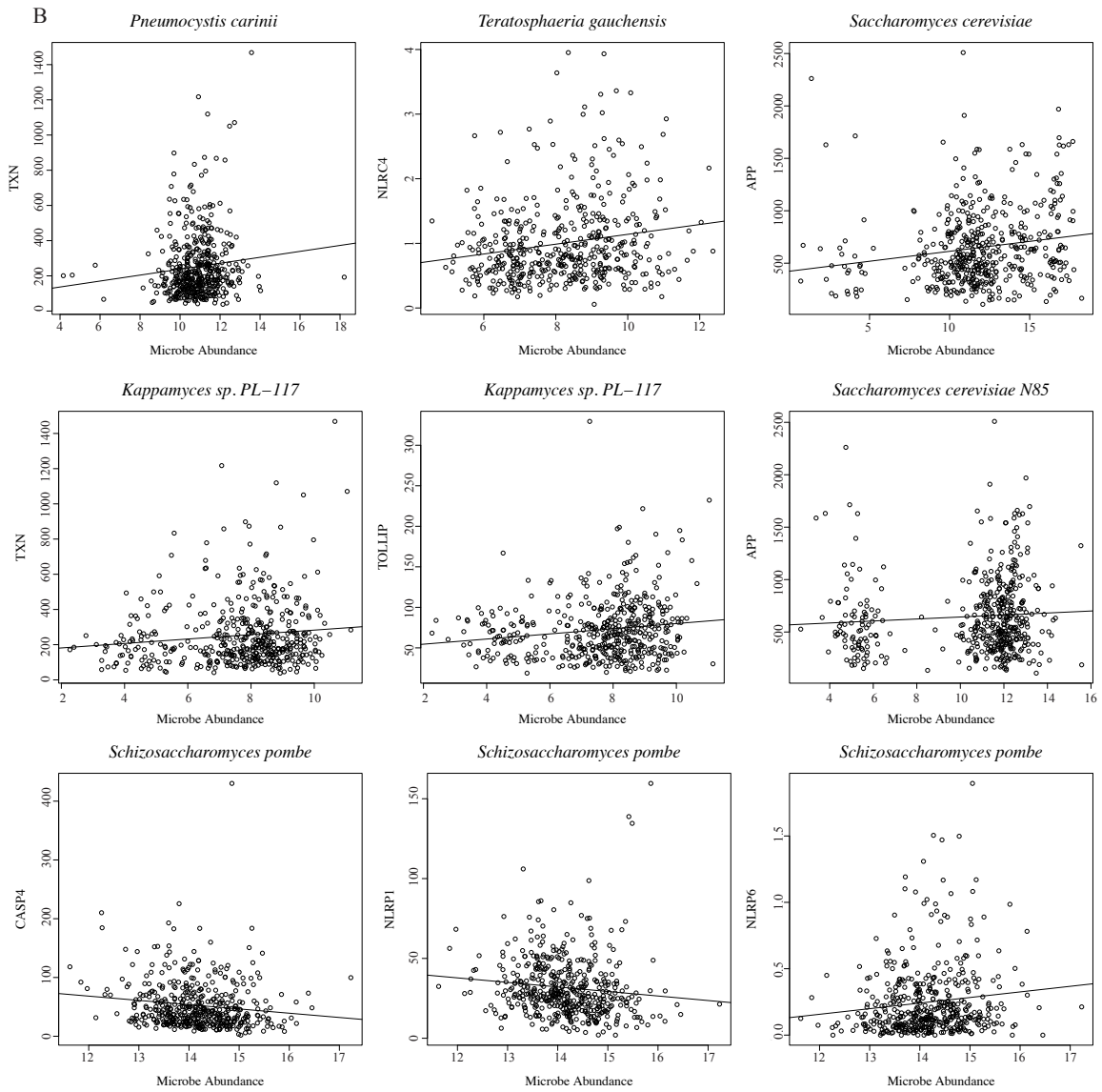
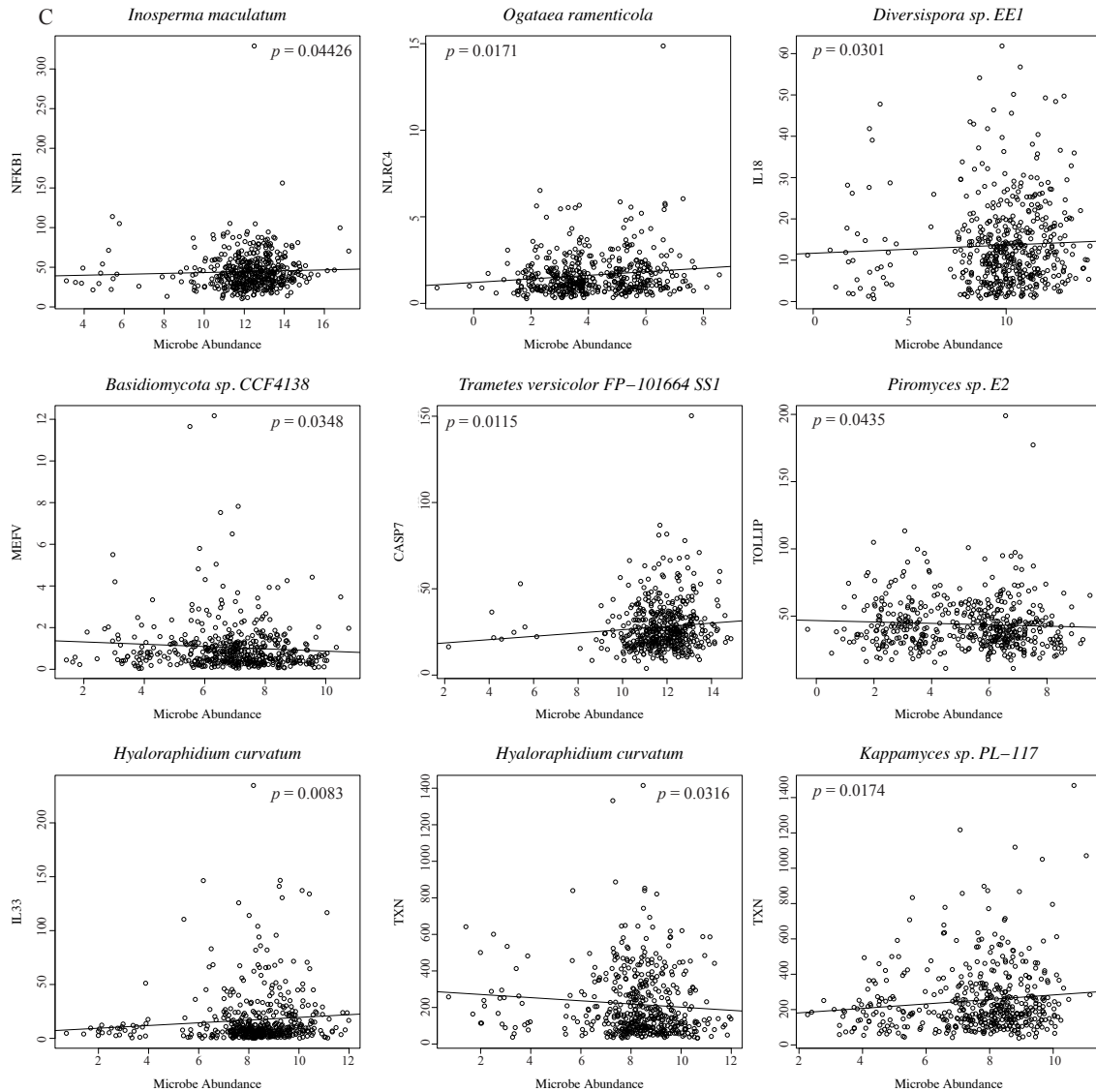


Figure 5 continued



### Correlation of Fungal Abundance to Immune Infiltration

Infiltration of immune cells into a tumor is often predictive of cancer outcomes. I therefore wanted to determine the association between fungal abundances and immune infiltration. I used CIBERSORTx software to determine the immune cell populations from tissue samples, and I used the Kruskal-Wallis test to examine the association between fungal abundances and the infiltration of 22 immune cell types. Of these 22 cell

types, 20 were associated with fungal abundances. In HNSC samples, the infiltration of resting CD4 T cells was associated with the greatest variety of fungi at 139. The immune cell types with infiltration values associated with the next greatest variety of fungal abundances were M2 macrophages with 77, activated mast cells with 57, neutrophils with 49, and activated NK cells with 43. In LUSC samples, the infiltration of B cells was associated with the greatest variety of fungal species at 125, followed by M0 macrophages at 93, resting NK cells at 72, mast cells at 59, and eosinophils at 47 (Figure 6A).

In HNSC samples, M2 macrophages tended to have higher tumor infiltration in samples with higher *Teratosphaeria gauchensis* abundance. *Teratosphaeria gauchensis* also had higher abundances in samples with greater infiltration of resting CD4 memory T cells. *Pneumocystis carinii* tended to have lower abundances in samples with lower infiltration of both M0 macrophages and resting CD4 memory T cells. *Saccharomyces cerevisiae* N85 had higher abundances in samples with greater infiltration of monocytes, M0 macrophages, and M2 macrophages. *Saccharomyces cerevisiae* had lower abundances in samples with greater infiltration of T follicular helper cells (Figure 6B).

In LUSC samples, resting NK cells tended to have lower tumor infiltration in samples with higher abundances of *Ogataea ramenticola* and *Hyaloraphidium curvatum*. M0 macrophages tended to have lower tumor infiltration in samples with higher abundances of *Z. bailii* CLIB 213 and *Hyaloraphidium curvatum*. *T. versicolor* FP-101664 SSI had higher abundances in samples with greater infiltration of CD8 T cells. *Piromyces* sp. E2 had lower abundances in patients with greater infiltration of M1 macrophages (Figure 6C).



Both HNSC and LUSC samples had fungi with increased abundance associated with increased and decreased infiltration of different immune cell types. This indicates that influencing immune cell infiltration is a plausible mechanism by which fungal abundances could influence the cancer immune response and cancer outcomes.

Figure 6 Correlation of fungal abundance to immune cell populations. (A) Bar plot of the number of fungi correlated to immune cell types. (B) Box plots showing correlation of fungal abundance to immune cell types in HNSC. (C) Box plots showing correlation of fungal abundance to immune cell types in LUSC. The outliers have been represented by °. Cibersortx was used to estimate immune cell populations in patient samples, and thereafter, Kruskal-Wallis test was used to find associations between immune cell types and fungal abundance. Significant correlations determined by  $p < 0.05$ .

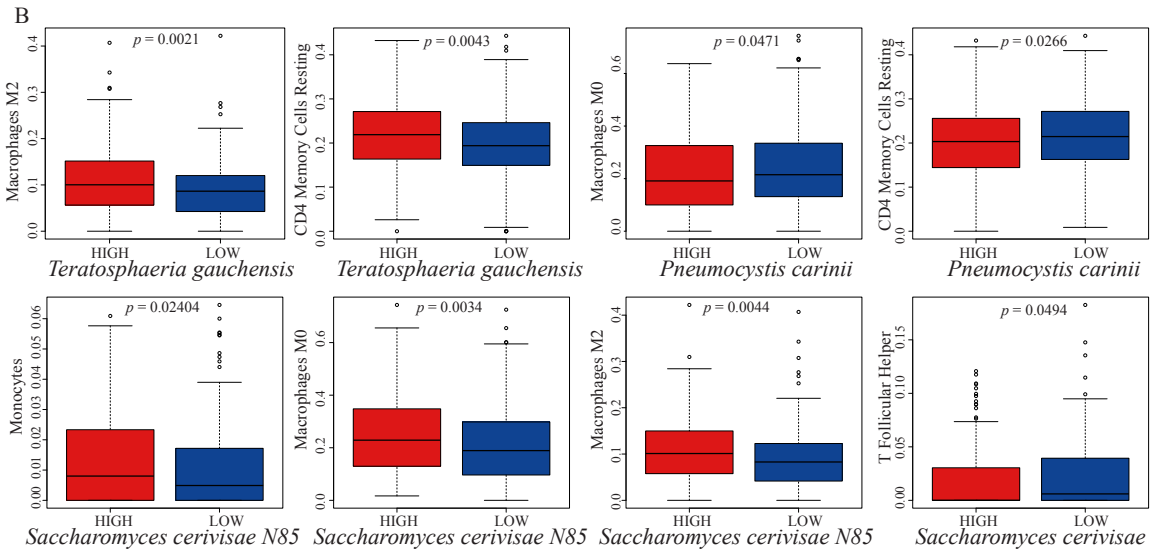
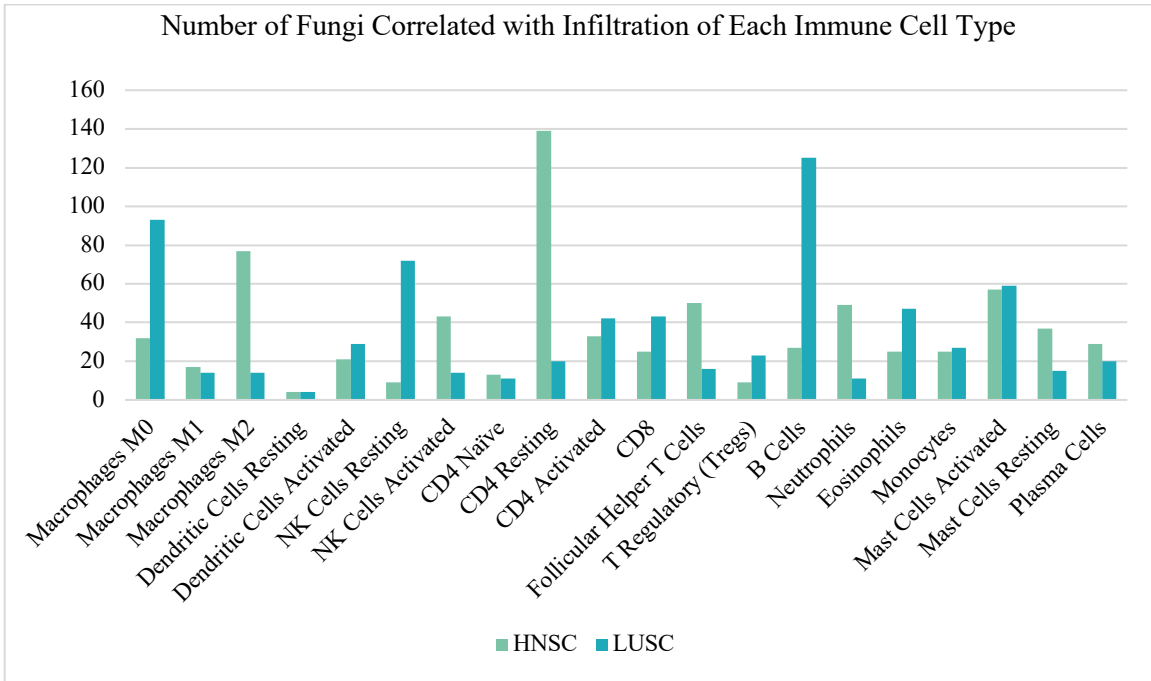
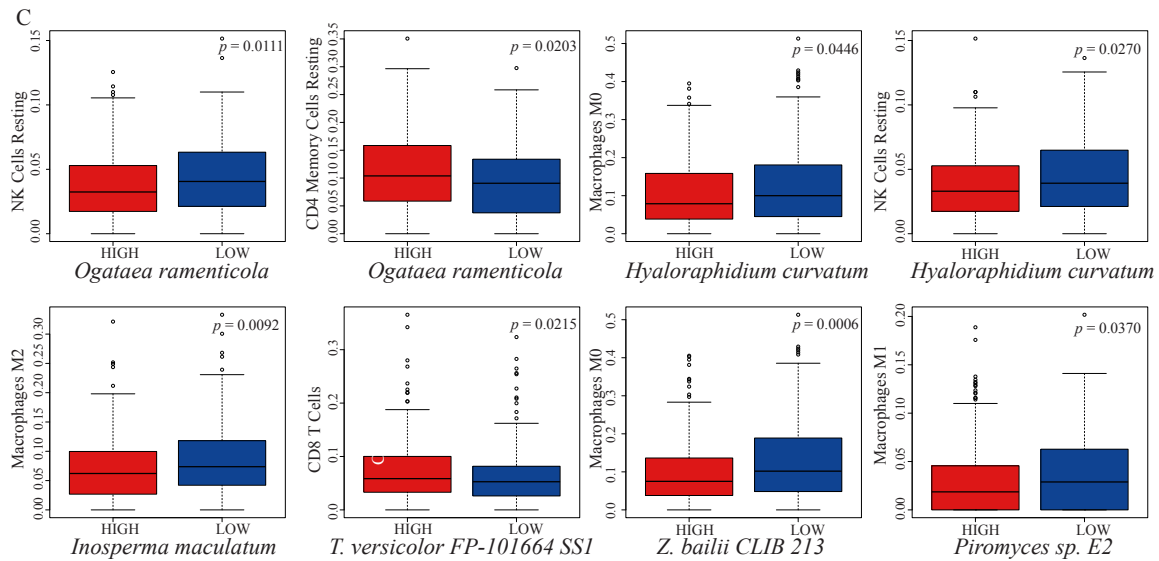


Figure 6 continued



### Correlation of Fungal Abundance to Inflammasome-Related Pathways

Many inflammasome genes are part of gene pathways. Looking at the overall enrichment of a pathway may elucidate relationships that would not be made clear by focusing on a single gene. I used gene set enrichment analysis (GSEA) to determine the association between fungal abundances and the enrichment of inflammasome-associated gene sets. In HNSC samples, seven fungi were significantly associated with the enrichment of inflammasome gene sets. In LUSC, 17 fungi were significantly associated with enrichment of inflammasome gene sets. In both HNSC and LUSC, only two gene sets were found to be significantly associated with fungi. These were REACTOME\_INFLAMMASOMES [45] and REACTOME\_THE\_NLRP3\_INFLAMMASOME [46].

In HNSC patients, abundance of *Renispora flavissima* tended to be higher when REACTOME\_INFLAMMASOMES was enriched. Abundance of *Monascus pilosus* tended to be higher when REACTOME\_THE\_NLRP3\_INFLAMMASOME was

enriched (Figure 7A). In LUSC patients, abundance of *Arthrotritys iridis* tended to be lower when REACTOME\_THE\_NLRP3\_INFLAMMASOME was enriched. Abundance of *Syncephalastrum monosporum* var. *pluriproliferum* tended to be higher when REACTOME\_THE\_NLRP3\_INFLAMMASOME was enriched (Figure 7B).

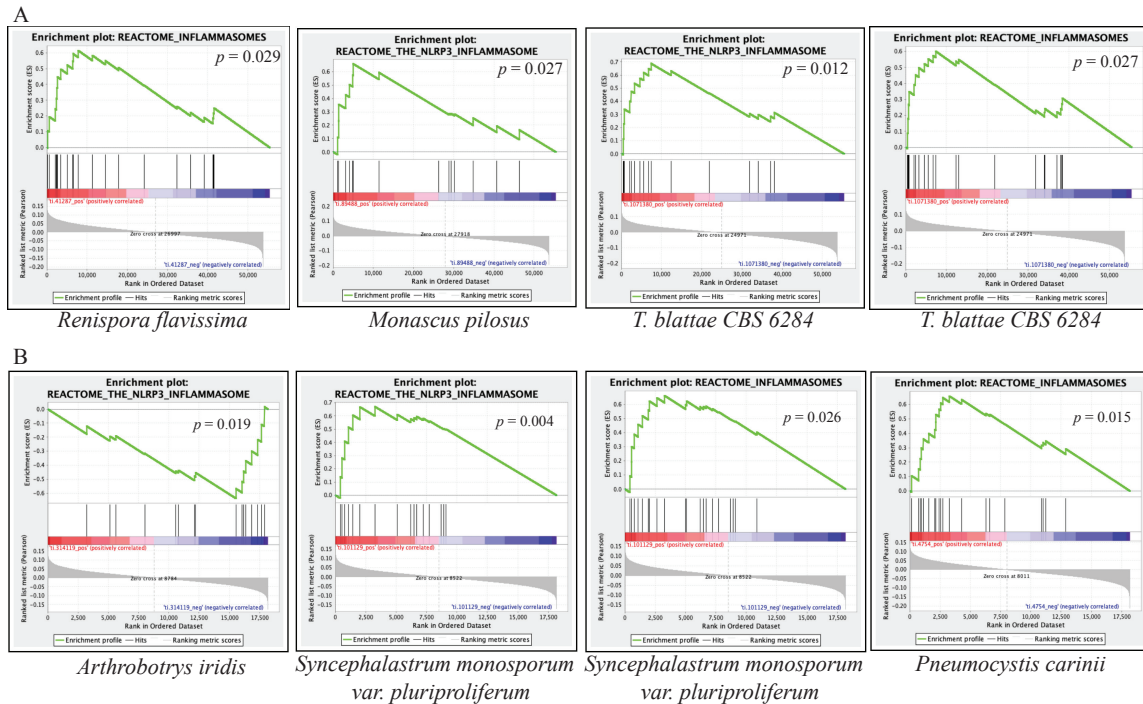


Figure 7 The association of fungal abundance to inflammasome-related pathways using GSEA ( $p < 0.05$ ). (A) Enrichment plots showing upregulated pathways in HNSC. (B) Enrichment plots showing downregulated (first plot) and upregulated pathways in LUSC.

## Chapter 4: Discussion

Cancers are a group of diseases that involve rapid, uncontrolled cell division. While we have learned much about the role of gene dysregulation in tumorigenesis, and major signaling pathways associated with cancer, many aspects of the disease are only now being considered. The role of the microbiome in cancer, for instance, has been studied in the last two decades and our understanding of the bacterial microbiome, and that of virus-associated cancers has also improved. The fungal mycobiome deserves our attention both in terms of identifying direct drivers of cancers as well as fungi that might be potential biomarkers of cancer and those that might be opportunistic in cancer patients.

Since fungal pathogen associated molecular patterns or PAMPs trigger the activation of inflammasomes, this is one area that deserves a closer look. If fungi were influencing cancer outcomes by dysregulating inflammasome genes, one would expect to find fungi that were differentially abundant in cancer tissue compared to normal tissue. One would also expect to find fungi with abundances associated with important cancer outcomes such as survival, pathologic T, pathologic M, and pathologic N. In addition, one would expect to find fungal abundances correlated with dysregulation of inflammasome genes and pathways. Identifying gene dysregulation of inflammasome-related genes and their correlations to fungal abundance can help elucidate important fungi and inflammasome-related genes in cancer. In this study, I investigated the mycobiome and the dysregulation of inflammasome-related genes in cancer. I found many fungi to be differentially significantly abundant in both HNSC and LUSC samples. Further analysis showed correlations between fungi and survival and clinically significant

factors. I also found multiple fungal species correlated to inflammasome-related genes, infiltration of immune cell types, and fungi that were correlated to inflammasome-related pathways.

Differential abundance analysis of HNSC and LUSC samples yielded 33 and 51 significant correlations respectively. Multiple fungi were found to be not only differentially significantly abundant, but also associated with patient survival, clinical variables, inflammasome-related genes, and the infiltration of immune cells. These fungi are of particular interest in the context of the mycobiome and immune response in HNSC and LUSC.

*Saccharomyces cerevisiae* was differentially abundant in both HNSC and LUSC, indicating that it could play a role in cancer. It had lower median abundance in cancer tissue than in adjacent normal tissue. This relationship was true in both HNSC patients and LUSC patients. This suggests that greater *S. cerevisiae* abundances are associated with decreased HNSC and LUSC cancer progression. However, in HNSC samples, *S. cerevisiae* abundance was correlated with expression of the APP gene, which is associated with cell growth and proliferation. Furthermore, HNSC patients with greater *S. cerevisiae* abundances had lower median tumor infiltration of T follicular helper cells than did HNSC patients with higher *S. cerevisiae* abundances. Infiltration of T follicular helper cells has been associated with better cancer outcomes and survival [50, 51]. If increased *S. cerevisiae* abundance did indeed decrease cancer progression, these results would be unexpected. Thus, the relationship between *S. cerevisiae* abundance and cancer progression is unclear. However, several strains of *S. cerevisiae* were also identified as being associated with cancer.

*Saccharomyces cerevisiae* N85 was also differentially abundant in both HNSC and LUSC cancer samples compared with adjacent normal tissue. This means that it could play a role in cancer and is a good candidate for further exploration. *S. cerevisiae* N85 had lower median abundances in normal tissue than cancer tissue. The fact that the direction of the association was the same in both HNSC and LUSC supports the case that *S. cerevisiae* N85 is associated with cancer progression. Furthermore, higher abundances of *S. cerevisiae* N85 were found to be associated with decreased survival in LUSC patients. This also supports the case that *S. cerevisiae* N85 is associated with cancer progression and shows that this fungus is associated with worse cancer outcomes. *S. cerevisiae* N85 was also positively correlated with expression of APP in HNSC patients. The APP gene is part of the NLRP3 inflammasome pathway, and it has been shown to be positively associated with increased cell growth and proliferation. Furthermore, higher abundances of *S. cerevisiae* N85 was associated with higher infiltration of monocytes, M0 macrophages, and M2 macrophages in HNSC. M2 macrophages are immunosuppressive and could therefore contribute to decreasing the immune response to the tumor. Together, these data suggest that higher *S. cerevisiae* N85 abundances contribute to progression of HNSC and lower survival of HNSC patients by upregulating APP and increasing tumor infiltration of M2 macrophages.

Another fungus that was differentially abundant in both HNSC and LUSC cancer tissue compared with normal tissue was *Kappamyces* sp. PL-117. Like *S. cerevisiae* N85, *Kappamyces* sp. PL-117 had lower median abundances in normal tissue than cancer tissue. Once again, the direction of the association was the same between the two cancers, supporting the conclusion that an association exists between increased *Kappamyces* sp.



*PL-117* abundance and cancer progression. *Kappamyces sp. PL-117* abundance was also found to be associated with pathologic N in HNSC patients. Pathologic N is a measure of the spread of cancer to lymph nodes. HNSC patients in the group with the greatest spread of cancer to lymph nodes had the highest median *Kappamyces sp. PL-117* abundance. *Kappamyces sp. PL-117* abundance was positively correlated with TOLLIP expression in HNSC. TOLLIP is a gene that regulates inflammatory signaling. Increased TOLLIP expression has been found to promote inflammation-associated colorectal cancer [52]. *Kappamyces sp. PL-117* abundance was also positively correlated with TXN expression. This positive correlation is present in both HNSC and LUSC. TXN is important for activation of the NLRP3 inflammasome and NF- $\kappa$ B binding of DNA [53]. Increased TXN expression is also associated with worse prognosis in clear cell renal cell carcinoma [54]. Therefore, increased *Kappamyces sp. PL-117* abundance may lead to cancer progression and worse cancer outcomes through upregulation of TXN and TOLLIP.

*Pneumocystis carinii* (also known as *Pneumocystis jirovecii*) is a fungus that causes Pneumocystis pneumonia or PCP. This is a dangerous infection especially in people with HIV/AIDS and other immunocompromised individuals. This fungus was differentially abundant in HNSC. *P. carinii* had a higher median abundance in HNSC cancer samples than in adjacent normal tissue. This suggests that increased *P. carinii* abundances contribute to cancer progression. This is supported by the fact that HNSC patients with high abundances of *P. carinii* tended to have lower survival than those with low *P. carinii* abundances. *P. carinii* abundance in HNSC patients was also correlated with expression of TXN. HNSC patients with higher *P. carinii* abundances also had lower median tumor infiltration of both M0 macrophages and resting CD4 memory cells.

Together, these findings suggest that increased *P. carinii* abundances in HNSC decrease patient survival and contribute to cancer progression by upregulating TXN and decreasing infiltration of M0 macrophages and resting CD4 memory cells. Additionally, the REACTOME\_INFLAMMASOMES pathway tended to be enriched in LUSC patients with higher *P. carinii* abundances.

*Schizosaccharomyces pombe* was another fungus found to be differentially abundant in HNSC patients. It had higher median abundance in cancer tissue compared to adjacent normal tissue, indicating that increased abundance is associated with cancer progression. HNSC patients with higher *S. pombe* abundances also tended to have lower survival than those with lower *S. pombe* abundances, so increased *S. pombe* abundance is associated with worse cancer outcomes. *S. pombe* abundance was negatively correlated with CASP4 expression. CASP4 is important to the activation of the NLRP3 [55] and NLRP6 [56] inflammasome. Additionally, activation of CASP4 can induce pyroptosis [57] and apoptosis [58]. *S. pombe* abundance was also negatively correlated with expression of NLRP1 and positively correlated with expression of NLRP6. NLRP1 is important for the inflammation and pyroptosis responses. Decreased expression of NLRP1 has been found to be associated with poor cancer prognosis, but NLRP1 has also been shown to promote tumor growth and suppress apoptosis [59]. Together, these results suggest that increased *S. pombe* abundance could lead to worse cancer outcomes in HNSC patients by downregulating expression of CASP4 and possibly NLRP1. However, *S. pombe* was also associated with HPV status and smoking status. Patients who were HPV positive tended to have higher *S. pombe* abundances than those who were HPV negative. Smoking patients also tended to have higher *S. pombe* abundances than

nonsmoking patients. Thus, the decreased patient survival and gene dysregulations may simply be linked to HPV infection or smoking rather than *S. pombe* abundance.

*Teratosphaeria gauchensis* abundance was associated with pathologic N stage in HNSC patients. Patients in the group with the greatest spread of cancer to lymph nodes had a higher median *T. gauchensis* abundance than did other groups. Thus, *T. gauchensis* could contribute to cancer spread. Abundance of *T. gauchensis* was also positively correlated with expression of NLRC4 in HNSC samples. This gene has been found to be upregulated in some cancers and downregulated in others [60]. Additionally, HNSC patients with higher abundances of *T. gauchensis* had greater median tumor infiltration of M2 macrophages, which could decrease the immune response to the tumor. However, patients with higher abundances of *T. gauchensis* also had greater median tumor infiltration of resting CD4 memory cells. Overall, these results suggest that increased *T. gauchensis* abundance could contribute to HNSC progression and spread by upregulating NLRC4 and increasing tumor infiltration of M2 macrophages.

*Ogatea ramenticola*, a methylotropic yeast, was a fungus found to be differentially abundant in LUSC patients. It had higher median abundance in cancer samples than adjacent normal samples, so increased *O. ramenticola* abundance is associated with cancer progression. LUSC patients with high *O. ramenticola* abundances had greater resting NK cell infiltration and lower resting CD4 memory cell infiltration than patients with lower *O. ramenticola* abundances. Abundance of *O. ramenticola* was positively correlated with expression of NLRC4. NLRC4 has been found to be upregulated in some cancers and downregulated in others [5]. Therefore, increases in *O. ramenticola* abundance could contribute to LUSC by upregulating NLRC4.

LUSC patients with high abundances of *Zygosaccharomyces bailii* CLIB 213 tended to have lower survival rates than those with lower abundances. *Z. bailii* CLIB 213 abundance was also significantly associated with pathologic N stage in LUSC patients. Patients in the group with the greatest spread of cancer to lymph nodes had a higher median *Z. bailii* CLIB 213 abundance than did other groups. Patients with higher abundances of *Z. bailii* CLIB 213 also tended to have lower tumor infiltration of M0 macrophages than those with lower abundances. Together, these results indicate that increased *Z. bailii* CLIB 213 abundance is associated with worse LUSC outcomes and survival. *Z. bailii* CLIB 213 could contribute to cancer progression and decrease patient survival by decreasing infiltration of M0 macrophages and increasing spread of cancer to lymph nodes.

Another fungus significantly associated with patient survival was *Inosperma maculatum*. LUSC patients with high abundances of *I. maculatum* tended to have lower survival than those with lower *I. maculatum* abundances. *I. maculatum* abundance was also positively correlated with NFKB1 expression in LUSC samples. NFKB1 codes for a subunit of the NF- $\kappa$ B protein complex, which is involved in regulation of cell survival and inflammation and has been found to be upregulated in cancer [61]. NF- $\kappa$ B has also been found to promote proliferation, cell survival, and angiogenesis in cancers [62]. However, LUSC patients with higher abundances of *I. maculatum* had lower median tumor infiltration of M2 macrophages than patients with lower *I. maculatum* abundances. M2 macrophages tend to be immunosuppressive. Overall, however, the results suggest that increased *I. maculatum* abundances could contribute to lower LUSC survival rates by upregulating NFKB1.

These results indicate that multiple fungal species are statistically associated with HNSC and LUSC cancer landscape. The study found four fungi that were significant to both cancers, and several more that were unique to each cancer. In addition, I found these differentially abundant fungi to be correlated with inflammasome-related genes, fitting the hypothesis that inflammasomes are key factors in the immune response to fungi and the development of cancer. However, these results could also be explained by differential abundance of fungi arising from changes in the cancer microenvironment. For example, if fungal growth is substantially changed in hypoxic or inflamed tissue, then presence of cancer can influence fungal growth. This could also explain the correlations between cancer outcomes and fungal abundance. Future experiments could therefore focus on elucidating the extent to which differential fungal abundances influence cancer outcomes and cancer outcomes influence fungal growth. Another question raised by these results is whether the dysregulation of inflammasome genes is primarily in tumor cells or in infiltrating immune cells. The fungi and inflammasome-related genes found significant in this study can thus be used in future mechanistic studies of pathogen-gene interactions.

## Appendix

Table S1: List of *Aspergillus* fungi identified as potential laboratory fungal contaminants.

NCBI Taxonomy ID – Contaminants	Fungus Name
ti.176178	<i>Aspergillus pseudodeflectus</i>
ti.510516	<i>Aspergillus oryzae</i> RIB40
ti.341663	<i>Aspergillus terreus</i> FGSC A1156
ti.344612	<i>Aspergillus clavatus</i> NRRL 1
ti.331117	<i>Aspergillus fischeri</i> NRRL 181
ti.330879	<i>Aspergillus fumigatus</i> Af293
ti.227321	<i>Aspergillus nidulans</i> FGSC A4

Table S2: List of fungi identified as potential contaminants by R package *decontam*.

Taxonomy ID – List of Contaminants	Fungus Name
ti.5007	<i>Brettanomyces bruxellensis</i>
ti.1280837	<i>Meira miltonrushii</i>
ti.40135	<i>Nosema bombi</i>
ti.5158	<i>Ceratocystis fimbriata</i>
ti.1305999	<i>fungal sp. JF58</i>
ti.1294372	<i>Saccharomyces cerevisiae YJM1439</i>
ti.28550	<i>Schwanniomyces etchellsii</i>
ti.178527	<i>Boletopsis leucomelaena</i>
ti.290209	<i>Dacrymyces sp. FPL8953</i>
ti.253819	<i>uncultured Agaricomycetes</i>
ti.1294317	<i>Saccharomyces cerevisiae YJM627</i>
ti.87269	<i>Umbilicaria rossica</i>
ti.379019	<i>Sordaria sp. JP63</i>
ti.1049725	<i>uncultured Glomeraceae</i>
ti.1305977	<i>fungal sp. JF38</i>
ti.1305991	<i>fungal sp. JF50</i>
ti.1294368	<i>Saccharomyces cerevisiae YJM1418</i>
ti.984090	<i>Mallocybe pygmaea</i>
ti.747082	<i>uncultured Pichia</i>
ti.164538	<i>Tetracladium marchalianum</i>
ti.191512	<i>Anaeromyces sp. W-98</i>
ti.1434223	<i>Parateratosphaeria bellula</i>
ti.310488	<i>Arthroderma melis</i>
ti.80646	<i>Boletinellus merulioides</i>
ti.86052	<i>Neophaeococcomyces catenatus</i>
ti.1636276	<i>Pochonia sp. CBS 634.75</i>
ti.1266744	<i>Talaromyces purpureogenus</i>
ti.5507	<i>Fusarium oxysporum</i>
ti.72558	<i>Sporisorium reilianum</i>
ti.1056129	<i>Brachyalara straminea</i>
ti.34458	<i>Ganoderma boninense</i>
ti.311114	<i>Torpedospora radiata</i>
ti.78921	<i>Tieghemomyces parasiticus</i>
ti.530120	<i>Parasola lilatincta</i>
ti.5191	<i>Ascobolus immersus</i>

Table S3: List of Inflammasome-Related genes included in analyses.

AIM2	MEFV	NOD1
APP	NACHT	NOD2
ASC	NAIP	P2RX7
BLC2	NEK7	PANX1
BLC2L1	NFKB1	PSTPIP1
CARD8	NFKB1A	PYCARD
CASP1	NFKB2	PYD
CASP4	NLR1	PYHIN
CASP5	NLRA	RELA
CASP7	NLRB	RIG1
CASP8	NLRC2	SUGT1
CIITA	NLRC4	TLR1
HBR3	NLRC5	TLR7
HSP90AB1	NLRP1	TNF
IFI16	NLRP1-13	TNFAIP3
IFNB1	NLRP12	TOLLIP
IL18	NLRP2	TXN
IL1B	NLRP3	TXNIP
IL1RL1	NLRP6	AIM2
IL33	NLRP7	
IPAF	NLRX1	



## References

1. *Erratum: Global cancer statistics 2018: GLOBOCAN estimates of incidence and mortality worldwide for 36 cancers in 185 countries.* CA Cancer J Clin, 2020. **70**(4): p. 313.
2. *U.S. Cancer Statistics Working Group. U.S. Cancer Statistics Data Visualizations Tool, based on 2020 submission data (1999-2018).* 2021 [cited 2022 4/2/2022]; Available from: [www.cdc.gov/cancer/dataviz](http://www.cdc.gov/cancer/dataviz).
3. Fan, X., Peters, B.A., Jacobs, E. J., Gapstur, S. M., Purdue, M. P., Freedman, N. D., Alekseyenko, A. V., Wu, J., Pei, Z., Hayes, R. B., Ahn, J., *Drinking alcohol is associated with variation in the human oral microbiome in a large study of American adults.* Microbiome, 2018. **6**(1): p. 59.
4. Blot, W.J., McLaughlin, J. K., Winn, D. M., Austin, D. F., Greenberg, R. S., Preston-Martin, S., Bernstein, L, Schoenberg, J. B., Stemhagen, A., Fraumeni, J. F., *Smoking and drinking in relation to oral and pharyngeal cancer.* Cancer Res, 1988. **48**(11): p. 3282-7.
5. Chen, Y.J., Chang, J. T., Liao, C. T., Wang, H. M., Yen, T. C., Chiu, C. C., Lu, Y. C., Li, H. F., Cheng, A. J., *Head and neck cancer in the betel quid chewing area: recent advances in molecular carcinogenesis.* Cancer Sci, 2008. **99**(8): p. 1507-14.
6. Amaya Arbeláez, M.I., de Paula E. S., Navegante, G., Valente, V., Barbugli, P. A., Vergani, C. E., *Proto-Oncogenes and Cell Cycle Gene Expression in Normal and Neoplastic Oral Epithelial Cells Stimulated With Soluble Factors From Single and Dual Biofilms of.* Front Cell Infect Microbiol, 2021. **11**: p. 627043.
7. Martins, D., F. Mendes, and F. Schmitt, *Microbiome: A Supportive or a Leading Actor in Lung Cancer?* Pathobiology, 2021. **88**(2): p. 198-207.
8. Cukic, V., *The Association Between Lung Carcinoma and Tuberculosis.* Med Arch, 2017. **71**(3): p. 212-214.
9. Brown, J.S., Hussell, T., Gilliland, S. M., Holden, D. W., Paton, J. C., Ehrenstein, M. R., Walport, M. J., Botto. M., *The classical pathway is the dominant complement pathway required for innate immunity to Streptococcus pneumoniae infection in mice.* Proc Natl Acad Sci U S A, 2002. **99**(26): p. 16969-74.
10. Rus, H., C. Cudrici, and F. Niculescu, *The role of the complement system in innate immunity.* Immunol Res, 2005. **33**(2): p. 103-12.
11. Barton, G.M., *A calculated response: control of inflammation by the innate immune system.* J Clin Invest, 2008. **118**(2): p. 413-20.

12. Horiguchi, H., Loftus, T., J., Hawkins, R. B., Raymond, S. L., Stortz, J. A., Hollen, M. K., Weiss, B. P., Miller, E. S., Bihorac, A., Larson, S. D., Mohr, A. M., Brakenridge, S. C., Tsujimoto, H., Ueno, H., Moore, F. A., Moldawer, L. L., Efron, P. A., *Innate Immunity in the Persistent Inflammation, Immunosuppression, and Catabolism Syndrome and Its Implications for Therapy*. Front Immunol, 2018. **9**: p. 595.
13. Erwig, L.P. and P.M. Henson, *Immunological consequences of apoptotic cell phagocytosis*. Am J Pathol, 2007. **171**(1): p. 2-8.
14. Zhao, H., Wu, L., Yan, G., Chen, Y., Zhou, M., Wu, Y., Li, Y., *Inflammation and tumor progression: signaling pathways and targeted intervention*. Signal Transduct Target Ther, 2021. **6**(1): p. 263.
15. El-Kenawi, A. and B. Ruffell, *Inflammation, ROS, and Mutagenesis*. Cancer Cell, 2017. **32**(6): p. 727-729.
16. Valavanidis, A., Vlachogianni, T., Fiotakis, K., Loridas, S., *Pulmonary oxidative stress, inflammation and cancer: respirable particulate matter, fibrous dusts and ozone as major causes of lung carcinogenesis through reactive oxygen species mechanisms*. Int J Environ Res Public Health, 2013. **10**(9): p. 3886-907.
17. Cui, J., Chen, Y., Wang, H. Y., Wang, R. F., *Mechanisms and pathways of innate immune activation and regulation in health and cancer*. Hum Vaccin Immunother, 2014. **10**(11): p. 3270-85.
18. Malik, A. and T.D. Kanneganti, *Inflammasome activation and assembly at a glance*. J Cell Sci, 2017. **130**(23): p. 3955-3963.
19. Tsuchiya, K., Hosojima, S., Hara, H., Kushiyama, H., Mahib, M. R., Kinoshita, T., Suda, T., *Gasdermin D mediates the maturation and release of IL-1 $\alpha$  downstream of inflammasomes*. Cell Rep, 2021. **34**(12): p. 108887.
20. Man, S.M., R. Karki, and T.D. Kanneganti, *Molecular mechanisms and functions of pyroptosis, inflammatory caspases and inflammasomes in infectious diseases*. Immunol Rev, 2017. **277**(1): p. 61-75.
21. Huang, C.F., Chen, L., Li, Y. C., Wu, L., Yu, G. T., Zhang, W. F., Sun, Z. J., *NLRP3 inflammasome activation promotes inflammation-induced carcinogenesis in head and neck squamous cell carcinoma*. J Exp Clin Cancer Res, 2017. **36**(1): p. 116.
22. He, Q., Fu, Y., Tian, D., Yan, W., *The contrasting roles of inflammasomes in cancer*. Am J Cancer Res, 2018. **8**(4): p. 566-583.

23. Karki, R., S.M. Man, and T.D. Kanneganti, *Inflammasomes and Cancer*. *Cancer Immunol Res*, 2017. **5**(2): p. 94-99.
24. Gajewski, T.F., H. Schreiber, and Y.X. Fu, *Innate and adaptive immune cells in the tumor microenvironment*. *Nat Immunol*, 2013. **14**(10): p. 1014-22.
25. Fitzgerald, D.C., Meade, K. G., McEvoy, A. N., Lillis, L., Murphy, E. P., MacHugh, D. E., Baird, A. W., *Tumour necrosis factor-alpha (TNF-alpha) increases nuclear factor kappaB (NFkappaB) activity in and interleukin-8 (IL-8) release from bovine mammary epithelial cells*. *Vet Immunol Immunopathol*, 2007. **116**(1-2): p. 59-68.
26. Liu, T., Zhang, L., Joo, D., Sun, S., *NF-κB signaling in inflammation*. *Signal Transduction and Targeted Therapy*, 2017. **2**: p.17023-.
27. Groth, C., Hu., X., Weber, R., Fleming, V., Altevogt, P., Umansky, V., *Immunosuppression mediated by myeloid-derived suppressor cells (MDSCs) during tumour progression*. *Br J Cancer*, 2019. **120**(1): p. 16-25.
28. Zhu, J., P.F. Petit, and B.J. Van den Eynde, *Apoptosis of tumor-infiltrating T lymphocytes: a new immune checkpoint mechanism*. *Cancer Immunol Immunother*, 2019. **68**(5): p. 835-847.
29. Vesty, A., Gear, K., Biswas, K., Radcliff, F. J., Taylor, M. W., Douglas, R. G., *Microbial and inflammatory-based salivary biomarkers of head and neck squamous cell carcinoma*. *Clin Exp Dent Res*, 2018. **4**(6): p. 255-262.
30. Weaver, D., Gago, S., Bromley, M., Bowyer, P., *The Human Lung Mycobiome in Chronic Respiratory Disease: Limitations of Methods and Our Current Understanding*. 2019, *Curr Fungal Infect Rep*. p. 109-119.
31. Kwon-Chung, K.J. and J.A. Sugui, *Aspergillus fumigatus--what makes the species a ubiquitous human fungal pathogen?* *PLoS Pathog*, 2013. **9**(12): p. e1003743.
32. Dambuja, I.M. and G.D. Brown, *Fungi accelerate pancreatic cancer*. *Nature*, 2019. **574**(7777): p. 184-185.
33. Godoy-Vitorino, F., Romaguera, J., Zhao, C., Vargas-Robles, D., Ortiz-Morales, G., Vazquez,-Sanchez, F., Vazquez-Sanchez, M., de la Garza-Casillas, M., Martinez-Ferrer, M., White, J. R., Bittinger, K., Dominguez-Bello, M. G., Blaser, M. J., *Cervicovaginal Fungi and Bacteria Associated With Cervical Intraepithelial Neoplasia and High-Risk Human Papillomavirus Infections in a Hispanic Population*. *Front Microbiol*, 2018. **9**: p. 2533.
34. Wang, N.J., Sanborn, Z., Arnett, K. L., Bayston, L. J., Liao, W., Proby, C. M., Leigh, I. M., Collisson, E. A., Gordon, P. B., Jakkula, L., Pennypacker, S., Zou,

- Y., Sharma, M., North, J. P., Vemula, S. S., Mauro, T. M., Neuhaus, I. M., Leboit, P. E., Hur, J. S., Park, K., Huh, N., Kwok, P. Y., Arron, S. T., Massion, P. P., Bale, A. E., Haussler, D., Cleaver, J. E., Gray, J. W., Spellman, P. T., South, A. P., Aster, J. C., Blacklow, S. C., Cho, R. J., *Loss-of-function mutations in Notch receptors in cutaneous and lung squamous cell carcinoma*. Proc Natl Acad Sci U S A, 2011. **108**(43): p. 17761-6.
35. Haider, M., Al-Rashed, F., Albaqsumi, Z., Alobaid, K., Alqabandi, R., Al-Mulla, F., Ahmad, R., *Induces Foaming and Inflammation in Macrophages through FABP4: Its Implication for Atherosclerosis*. Biomedicines, 2021. **9**(11).
36. Hernández-Santos, N. and S.L. Gaffen, *Th17 cells in immunity to Candida albicans*. Cell Host Microbe, 2012. **11**(5): p. 425-35.
37. Wang, W., Deng, Z., Wu, H., Zhao, Q., Li, T., Zhu, W., Wang, X., Tang, L., Wang, C., Cui, S. Z., Xiao, H., Chen, J., *A small secreted protein triggers a TLR2/4-dependent inflammatory response during invasive Candida albicans infection*. Nat Commun, 2019. **10**(1): p. 1015.
38. Hong, C., Manimaran, S., Shen, Y., Perez-Rogers, J. F., Byrd, A. L., Castro-Nallar, E., Crandall, K. A., Johnson, W. E., *PathoScope 2.0: a complete computational framework for strain identification in environmental or clinical sequencing samples*. Microbiome, 2014. **2**: p. 33.
39. Ritchie, M.E., Phipson, B., Wu, D., Hu, Y., Law, C. W., Shi, W., Smyth, G. K., *limma powers differential expression analyses for RNA-sequencing and microarray studies*. Nucleic Acids Res, 2015. **43**(7): p. e47.
40. Davis, N. M., Proctor, D. M., Holmes, S. P., Relman, D. A., Callahan, B. J., *Simple statistical identification and removal of contaminant sequences in marker-gene and metagenomics data*, P. D., Editor. 2017, *bioRxiv*.
41. Love, M.I., W. Huber, and S. Anders, *Moderated estimation of fold change and dispersion for RNA-seq data with DESeq2*. Genome Biol, 2014. **15**(12): p. 550.
42. Liberzon, A., A., Subramanian, A., Thorvaldsdottir, H., Tamayo, P., Mesirov, J. P., *Molecular signatures database (MSigDB) 3.0*. Bioinformatics, 2011. **27**(12): p. 1739-40.
43. Subramanian, A., Tamayo, P., Mootha, V. K., Mukherjee, S., Ebert, B. L., Gillette, M. A., Paulovich, A., Pomeroy, S. L., Golub, T. R., Lander, E. S., Mesirov, J. P., *Gene set enrichment analysis: a knowledge-based approach for interpreting genome-wide expression profiles*. Proc Natl Acad Sci U S A, 2005. **102**(43): p. 15545-50.

44. Chen, B., Khodadoust, M. S., Liu, C. L., Newman, A. M., Alizadeh, A. A., *Profiling Tumor Infiltrating Immune Cells with CIBERSORT*. *Methods Mol Biol*, 2018. **1711**: p. 243-259.
45. *PubChem Pathway Summary for Pathway R-HSA-622312, Inflammasomes*, *Source: Reactome*. 2004, National Center for Biotechnology Information.
46. *PubChem Pathway Summary for Pathway R-HSA-844456, The NLRP3 inflammasome*, *Source: Reactome*. National Center for Biotechnology Information.
47. Mirjalili, A., Parmoor, E., Moradi Bidhendi, S., Sarkari, B., *Microbial contamination of cell cultures: a 2 years study*. *Biologicals*, 2005. **33**(2): p. 81-5.
48. Shafiq, S.A. and Y.H. Aljuraissy, *Prevalence of Fungal Contamination in Some of Biology Department's Laboratories*. 2019. p. 36-39.
49. Davis, N.M., *Simple statistical identification and removal of contaminant sequences in marker-gene and metagenomics data*. *Microbiome*, 2018. **6**(1): p. 226.
50. Baumjohann, D. and P. Brossart, *T follicular helper cells: linking cancer immunotherapy and immune-related adverse events*. *J Immunother Cancer*, 2021. **9**(6).
51. Nurieva, R., Liu, Z., Gangadharan, A., Bieberkehazhi, S., Zhao, Y., Alekseev, A., *Function of T follicular helper cells in anti-tumor immunity*. 2019, *The Journal of Immunology*.
52. Begka, C., Pattaroni, C., Mooser, C., McCoy, K. D., Velin, D., Maillard, M. H., *Toll-Interacting Protein Regulates Immune Cell Infiltration and Promotes Colitis-Associated Cancer*. *iScience*, 2020. **23**(3): p. 100891.
53. Muri, J., Thut, H., Feng, Q., Kopf, M., *Thioredoxin-1 distinctly promotes NF- $\kappa$ B target DNA binding and NLRP3 inflammasome activation independently of Txnip*. *Elife*, 2020. **9**.
54. Ribback, S., Winter, S., Klatte, T., Scaeffeler, E., Gellert, M., Stuhler, V., Scharpf, M., Bedke, J., Burchardt, M., Schwab, M., Lillig, C. H., Kroeger, N., *Thioredoxin 1 (Trx1) is associated with poor prognosis in clear cell renal cell carcinoma (ccRCC): an example for the crucial role of redox signaling in ccRCC*. *World J Urol*, 2022. **40**(3): p. 739-746.
55. Sollberger, G., Strittmatter, G. E., Kistowska, M., French, L. E., Beer, H. D., *Caspase-4 is required for activation of inflammasomes*. *J Immunol*, 2012. **188**(4): p. 1992-2000.

56. Tian, X.X., Li, R., Liu, C., Liu, F., Yang, L. J., Wang, S. P., Wang, C. L., *NLRP6-caspase 4 inflammasome activation in response to cariogenic bacterial lipoteichoic acid in human dental pulp inflammation*. *Int Endod J*, 2021. **54**(6): p. 916-925.
57. Shi, J., Zhao, Y., Wang, K., Shi, X., Wang, Y., Huang, H., Zhuang, Y., Cal, T., Wang, F., Shao, F., *Cleavage of GSDMD by inflammatory caspases determines pyroptotic cell death*. *Nature*, 2015. **526**(7575): p. 660-5.
58. Hitomi, J., Katayama T., Eguchi, Y., Kudo, T., Taniguchi, M., Koyama, Y., Manabe, T., Yamagishi, S., Bando, Y., Imaizumi, K., Tsujimoto, Y., Tohyama, M., *Involvement of caspase-4 in endoplasmic reticulum stress-induced apoptosis and Abeta-induced cell death*. *J Cell Biol*, 2004. **165**(3): p. 347-56.
59. Shen, E., Han., Y., Cai, C., Liu, P., Chen, Y., Gao, L., Huang, Q., Shen, H., Zeng, S., He, M., *Low expression of NLRP1 is associated with a poor prognosis and immune infiltration in lung adenocarcinoma patients*. *Aging (Albany NY)*, 2021. **13**(5): p. 7570-7588.
60. Wen, J., Xuan, B., Liu, Y., Wang, L., He, L., Meng, X., Zhou, T., Wang, Y., *Updating the NLRC4 Inflammasome: from Bacterial Infections to Autoimmunity and Cancer*. *Front Immunol*, 2021. **12**: p. 702527.
61. Li, Y.Y., Chung, G. T., Lui, V. W., To, K. F., Ma, B. B., Chow, C., Woo, J. K., Yip, K. Y., Seo, J., Hui, E. P., Mak, M. K., Rusan, M., Chau, N. G., Or, Y. Y., Law, M. H., Law, P. P., Liu, Z. W., Ngan, H. L., Hau, P. M., Verhoeft, K. R., Poon, P. H., Yoo, S. K., Shin, J. Y., Lee, S. D., Lun, S. W., Jia, L., Chan, A. W., Chan, J. Y., Lai, P. B., Fung, C. Y., Hung, S. T., Wang, L., Chang, A. M., Chioesa, S. I., Hedberg, M. L., Tsao, S. W., van Hasselt, A. C., Chan, A. T., Grandis, J. R., Hammerman, P. S., Lo, K. W., *Exome and genome sequencing of nasopharynx cancer identifies NF- $\kappa$ B pathway activating mutations*. *Nat Commun*, 2017. **8**: p. 14121.
62. Xia, L., Tan, S., Zhou, Y., Lin, J., Wang, H., Oyang, L., Tian, Y., Liu, L., Su, M., Cao, D., Liao, Q., *Role of the NF $\kappa$ B-signaling pathway in cancer*. *Onco Targets Ther*, 2018. **11**: p. 2063-2073.